The EuroBiotech Journal
REVIEW
Biosensors

Point-of-Care Diagnostics: Molecularly Imprinted Polymers and Nanomaterials for Enhanced Biosensor Selectivity and Transduction

Daniel J. Denmark[a,b,c,d*], Subhra Mohapatra[a,c,e], Shyam S. Mohapatra[a,b,c,d*]

Abstract

Significant healthcare disparities resulting from personal wealth, circumstances of birth, education level, and more are internationally prevalent. As such, advances in biomedical science overwhelmingly benefit a minority of the global population. Point-of-Care Testing (POCT) can contribute to societal equilibrium by making medical diagnostics affordable, convenient, and fast. Unfortunately, conventional POCT appears stagnant in terms of achieving significant advances. This is attributed to the high cost and instability associated with conventional biorecognition: primarily antibodies, but nucleic acids, cells, enzymes, and aptamers have also been used. Instead, state-of-the-art biosensor researchers are increasingly leveraging molecularly imprinted polymers (MIPs) for their high selectivity, excellent stability, and amenability to a variety of physical and chemical manipulations. Besides the elimination of conventional bioreceptors, the incorporation of nanomaterials has further improved the sensitivity of biosensors. Herein, modern nanobiosensors employing MIPs for selectivity and nanomaterials for improved transduction are systematically reviewed. First, a brief synopsis of fabrication and wide-spread challenges with selectivity demonstration are presented. Afterward, the discussion turns to an analysis of relevant case studies published in the last five years. The analysis is given through two lenses: MIP-based biosensors employing specific nanomaterials and those adopting particular transduction strategies. Finally, conclusions are presented along with a look to the future through recommendations for advancing the field. It is hoped that this work will accelerate successful efforts in the field, orient new researchers, and contribute to equitable health care for all.

Keywords: molecularly imprinted polymer (MIP), biosensor, point-of-care testing (POCT), nanomaterial, transducer, bioreceptor

[a]James A Haley VA Hospital, Tampa, FL; [b]Taneja College of Pharmacy, [c]Center for Research and Education in Nanobioengineering, Departments of [d]Internal Medicine and [e]Molecular Medicine, Morsani College of Medicine, University of South Florida, Tampa, FL.

Co-Corresponding Authors: Daniel J. Denmark and Shyam S. Mohapatra
*Email: denmark@usf.edu and smohapat@usf.edu

DOI: 10.2478/ebtj-2020-0023

Introduction

While many individuals in post-industrial countries enjoy access to advanced healthcare, most people do not share the same privilege. Current times are unusual in that unprecedented gains in potent biomedicine coincide with significant, albeit varied, preventable mortality. Avoidable deaths increase (1, 2) as researchers learn to relate trends in a particular bioanalyte to the worsening of a corresponding condition. Consider the differing amounts of SARS-CoV-2 virus or antibody exhibited by critical COVID-19 patients compared to non-critical patients (3, 4), the relation between non-linear serum creatinine and impending kidney failure (5, 6), and the monitoring of lung transplant patients for immunosuppressant therapies (7, 8). At the same time, in an evaluation of 195 nations, populations with short average education, low fertility rates, and reduced income per capita have a higher incidence of death resulting from tetanus and measles (2), which are considered minor threats in advanced healthcare systems. In the United States of America where healthcare is not a basic human right, citizens must be employed or wealthy for consistent and quality access to physicians, hospitals, and medical diagnostics (9, 10). In particular, US patients with chronic medical conditions and the disabled experience

healthcare irregularities (11, 12). Mounting evidence indicates inequitable access to quality healthcare among varying populations categorized by socioeconomic status, ethnicity, and sexual orientation (13, 14). Fortunately, a methodology known as Point-of-Care Testing (POCT) has manifested that holds promise for resolving some of these concerns. POCT aims to bring biomedical diagnostics to all patients that are inexpensive, convenient, and faster than conventionally possible (15-18). Also, smartphone technology has proven invaluable for connecting relevant stakeholders like patients, physicians, and caregivers in a timely manner (19, 20). POCT efforts merged with smartphone advances allow for biosensors connected to the internet, contributing to timely, equitable, and affordable access to quality healthcare.

The trajectory of healthcare toward personalized medicine is realizing medical tests that are widely accessible, faster and more convenient, and low-cost with biosensors. These instruments selectively identify and sensitively quantify bioanalytes from a patient or environmental sample (21-24). An important aspect of biosensor operation is the sensitive quantification of bioanalyte concentration, after it is recognized, through transduction. Several categories of transduction exist, like electrochemical (ECM) (25, 26), optical (27, 28), magnetic (29, 30), thermometric (31, 32), and gravimetric (33, 34). Biosensors research is dominated by ECM and optical devices, but other strategies offer beneficial attributes for optimized strategy depending on the bioanalyte and application constraints. Biosensors rely on selective binding to recognize the analyte. Antibodies are predominant, but nucleic acids, enzymes, and cells have also been used for biorecognition. While conventional bioreceptors do achieve selectivity, they are expensive, have poor shelf-life, pose technical difficulties to implementation, and raise ethics concerns associated with animal exploitation (35-38).

Since recognition is integral to biosensor operation, an alternative strategy is wanted that achieves selectivity while mitigating the disadvantages linked with conventional biorecognition (39, 40). This motivates the development of molecularly imprinted polymers (MIPs) for biosensors applications (41-45). Compared to antibodies, MIPs usually exhibit a decreased limit of detection (LOD) and improved stability resulting in potential for sensor reuse (Table 1). MIPs are fabricated using the target analyte as a model during polymerization for selective binding sites in the polymer matrix, which have physical and chemical affinity for the intended bioanalyte, after the target is removed (46-48). A Web of Science search for the phrase "molecularly imprinted polymer" conveys the interest in this field (Fig. 1a). Besides biosensors, several other MIP applications exist, such as for cancer diagnosis and therapy (49-51), drug delivery (52-54), sample homogenization through chromatography (55-57), and environmental remediation (58-60). Despite excellent selectivity, low cost, and stability, the first MIPs presented challenges to effective biosensing. For one, MIPs are inherently insulating causing the inhibition of sensitivity. Furthermore, early MIPs suffered from poor mass transfer, or the incomplete removal or saturation of MIP matrix with a sample containing the target. This latter challenge resulted in sensitivity and reuse issues.

The societal metamorphoses of the past, brought on by the transformative textile, automobile, and computer revolutions, are similar to the recently begun nanotechnological era. Nanomaterials pervade our lives in the form of freshness indicators in food packaging (61-63), water repellents for electronic devices (64-66), additives in food stuffs (67-69), enhancers in solar cells (70-72), and in cosmetics (73-75). Biomedical research has benefited the most and progressed the furthest through nanotechnology. For example, magnetic nanoparticles are applied to targeted and triggered drug delivery (76-78), gold nanoparticles bind antibodies in conventional biosensing (79-81), and zinc oxide and titanium dioxide nanoparticles protect skin (82, 83). Solutions to the challenges MIPs originally presented have been found through MIP nanoformulations or by incorporating them with nanomaterials (46, 84, 85). Nanomaterials offer advantages over their micro- and bulk counterparts, such as improved surface area to volume ratio and functional, novel behavior that only manifests when electron quantum confinement is realized (86-89). These solutions are increasingly popular with researchers. A Web of Science literature search (Fig. 1b), for the phrase "molecularly imprinted polymer nanoparticle" reveals increasing publications and ci-

Table 1. MIP versus antibody performance. The first three columns demonstrate typical LOD decreases when antibodies are replaced with MIPs. The last four columns demonstrate robust MIP potential for regeneration, which is not possible when fragile antibodies are used.

Target Analyte	LOD % Decrease (-) or Increase (+)	Reference	Target Analyte	Times Regenerated	Signal Decrease (%)	Reference
Biotin	-52	39	CAP	5	7	112
Fumonisin B2	-76	39	BSA	4	8	95
Glucosamine	33	39	Artesunate	5	11	50
L-Thyroxine	-100	39	BHb	4	14	188

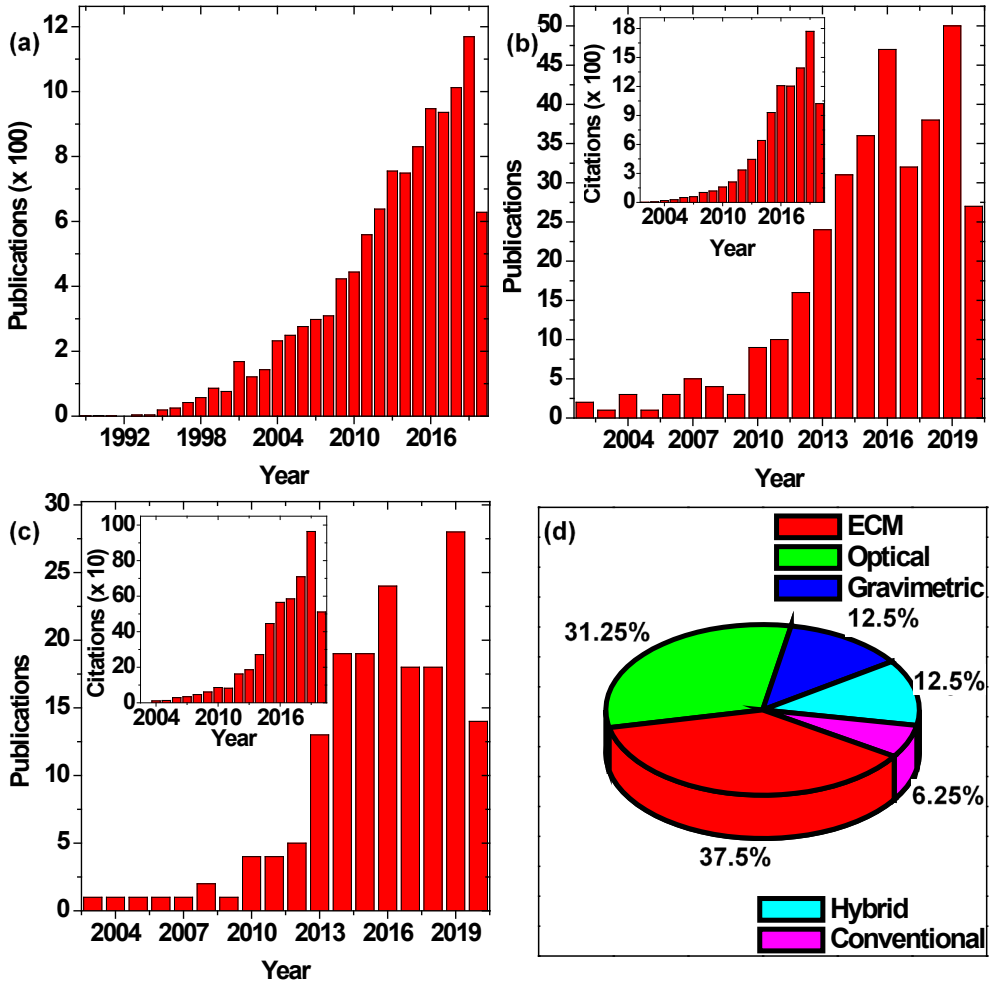

Figure 1. (a) Publications per year for the phrase "molecularly imprinted polymer." Since the maximum set size for the number of citations exceeded 10,000, Web of Science could not generate that data. **(b)** Publications per year for the phrase "molecularly imprinted polymer nanoparticle." The inset shows the citations per year for the same search. **(c)** Publications per year for the phrase "molecularly imprinted polymer nanoparticle" and the term "sensor." The inset shows the citations per year for the same search. **(d)** Relative occurrence of the transduction strategy of the sensors tabulated in this review. This data was extracted from Web of Science on July 14, 2020.

tations (inset) per year.

The urgent need for expanded POCT can be met with biosensors that abandon conventional biorecognition for nano-enhanced MIPs. Already this growing subset of biosensors research is apparent, as demonstrated by the Web of Science literature search for the phrase "molecularly imprinted polymer nanoparticle" and "sensor" (Fig. 1c). Herein, a methodical review of state-of-the-art nanobiosensors relying on MIP bioanalyte targeting is presented. Relevant reports within the past five years are identified and tabulated as note-worthy case studies. The field is viewed through two lenses for a robust perspective. First, a brief accounting of advances in biorecognition is presented. Next, case studies of nanobiosensors organized by component nanomaterials are discussed. Afterward, a parallel discussion is provided for different case studies, organized by transduction strategy. Even though some transduction strategies are more prevalent in the literature (Fig. 1d), this report evaluates them equally. Finally, a section dedicated to conclusions is presented with future directions for the field. It is hoped that this update to the field will pave the way to significant advances toward realizing affordable and equitable biodiagnostics. Throughout this work numerous acronyms are used (Table 2).

2. Molecularly imprinted Polymers (MIPs)

MIP advantages over conventional bioreceptors have resulted in commercialized products (90). Marketers of MIP-based products include Aspira Biosystems, Supelco, Oxonon, and Semorex. They have sold MIP-based products for protein arrays, solid phase extraction, HPLC, drug screening, and other sensors.

Since MIPs synthesis is already comprehensively detailed (41, 46-48, 85, 91-94), this review begins with brief foundational remarks that quickly shift to current considerations in the field. After MIPs are described, their fabrication is detailed in terms of their significant historical development through to

Table 2. Alphabetized list of acronyms used in this review.

Acronym	Word / Phrase	Acronym	Word / Phrase
AgNM	silver nanomaterial	MOF	metal organic framework
AuNM	gold nanomaterial	MWCNT	multi-walled carbon nanotube
BHb	bovine hemoglobin	NEMS	nano electromechanical systems
BSA	bovine serum albumin	NIP	non-imprinted polymer
CA-125	cancer antigen 125	NM	nanomaterial
CA-153	cancer antigen 153	NNI	National Nanotechnology Initiative
CAP	chloramphenicol	NP	nanoparticle
CEA	carcinoembryonic antigen	NSE	neuron-specific enolase
CL	chemiluminescence	PB	phosphate buffer
CNM	carbon nanomaterial	PBS	phosphate-buffered saline
CPX	ciprofloxacin	PGM	personal glucose meter
CPZ	chlorpromazine	p-NP	p-nonylphenol
cTnI	cardiac troponin I	POC	point-of-care
CuNC	copper nanocluster	POCT	point-of-care test(ing)
DA	dopamine	PSMA	prostate-specific membrane antigen
DLP	dansyl-L-phenylalanine	pTyr	tyrosine phosphopeptide
ECL	electrochemiluminesnce	PVDF	poly(vinylidene difluoride)
ECM	electrochemical	QCM	quartz crystal microbalance
ELISA	enzyme-linked immunosorbent assay	QD	quantum dot
GMR	giant magnetoresistance	R6G	rhodamine 6G
GO	graphene oxide	RAFT	reversible addition/fragmentation chain transfer
HPLC	high performance liquid chromatography	SA	salicylic acid
IOMNP	iron oxide magnetic nanoparticle	SAW	surface acoustic wave
LC-MS/MS	liquid chromatography tandem mass spectrometry	SCCA	squamous cell carcinoma antigen
LOD	limit of detection	SERS	surface enhances Raman spectroscopy
MA	methamphetamine	SNM	silica nanomaterials
MAA	methacrylic acid	SPR	surface plasmon resonance
MEMS	micro electromechanical systems	SQUID	superconducting quantum interfernce device
MIP	molecularly imprinted polymer	TCF	trichlorfon
MIPNP	molecularly imprinted polymer nanoparticle	TNM	titanium dioxide nanomaterials
MNP	magnetic nanoparticle	UPLC	ultra performance liquid chromatography

the modern variety. This section ends with a discussion of the various applications for a MIP-based biosensor.

2.1. Conventional Fabrication

The fundamental aspect of MIP operation is the creation of a selective pore for some analyte within a polymer's matrix. Ideally, the MIP pore readily binds the analyte and retains it until transduction can take place. It is desirable if the MIP is easily refreshed or recycled for future use through template removal (95). In general, MIP pores are realized via polymerization of a functional monomer in the presence of the target analyte. After fabrication the analyte should be easily removed in a process like elution leaving a custom binding site for the intended application. The result is an epitope having a physical shape that corresponds to the analyte's shape as well as chemical affinity for the analyte. (46)

MIP analyte binding can be covalent or noncovalent. Epitopes depending solely on covalent binding tend to be significantly more selective. Unfortunately, covalent epitopes are rigid in their production in that only a few suitable functional mono-

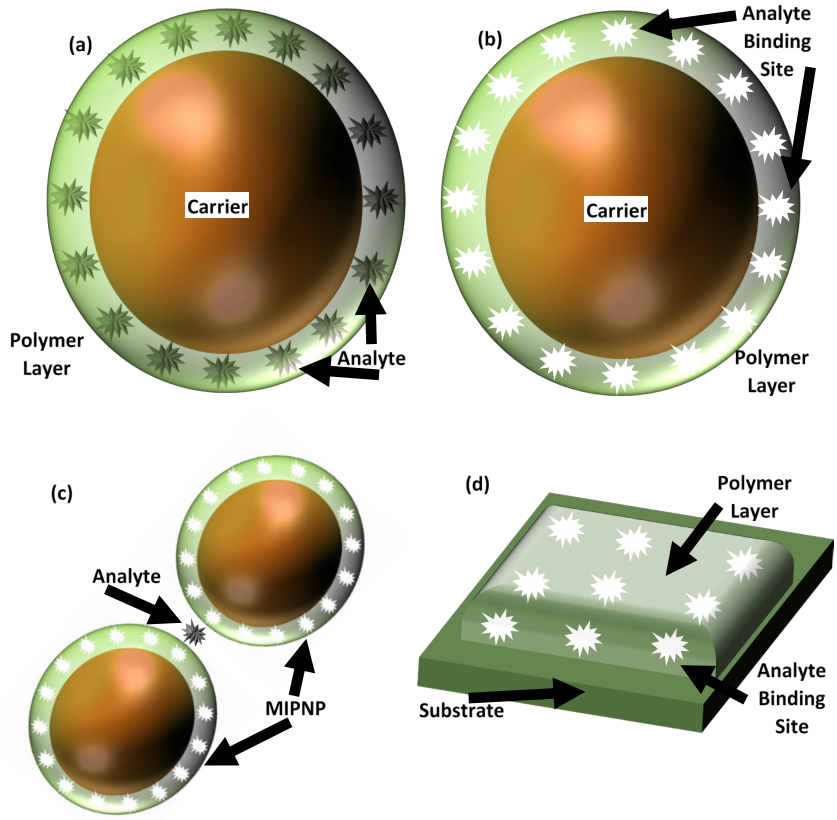

Figure 2. (a) Many MIPNP conformations assume a core-shell configuration, where the core NP composition varies depending on the intended function. The shell is often a nano-thin MIP layer for selective binding. Here, the template analyte is retained during polymerization. **(b)** Later, the analyte can be removed via elution, leaving binding sites complementary to the target analyte. **(c)** Selectivity can be enhanced by designing two different MIPNPs, as in (a) and (b), each for distinct parts of the analyte, thus realizing a sandwich immunoassay. **(d)** For homogeneous biosensing, a nano-thin MIP layer like an electrode, wave guide, or piezoelectric cantilever, can be deposited on the relevant substrate for selective binding.

mers are available. In noncovalent analyte recognition, a MIP and target can bind through π-π interactions, van der Waals forces, hydrogen bonding, and ionic interactions. (47)

A bulk MIP can be produced via free-radical polymerization and milled down to smaller sizes for simple fabrication. Unfortunately, the strategy results in a low selectivity MIP and excessive target analyte consumption. Noncovalent recognition is more accessible to most researchers due to facile execution. In addition, noncovalent binding and release tends to be faster, which is important in POCT. On the other hand, noncovalent recognition tends to result in less selective biosensors since the interactions are easier to disturb. (96)

2.2. Innovative Fabrication

Advanced MIP fabrication employs techniques like seed, suspension, precipitation, and emulsion polymerization (46). In particular, there is significant motivation to realize surface imprinting on some nanocarrier or substrate to maximize mass transfer (95, 97) (Fig. 2). This achieves effective diffusion of the analyte through the MIP matrix for rapid recognition and sensor refreshment. In addition, state-of-the-art MIP-based biosensors tend to realize a semicovalent strategy, or covalent templating followed by noncovalent sensor operation (96). Stimuli-responsive polymers are leveraged for the need for more functional monomers, protein recognition, and temperature responsive functionality (48, 52, 95, 98-102). The limited number of functional monomers is also addressed through computational prediction of monomers complementary to particular analytes and through novel chemical solutions, like repurposing silica as a monomer.

Before leaving the topic of MIP fabrication, it is instructive to highlight an unusual phenomenon in the literature. Efforts to realize a nanobiosensor with MIP binding are obligated to demonstrate analyte selectivity. This is often achieved by comparison of the device evaluation amongst samples containing the target analyte, chemical analogs, and potential interferents. Convincing data is characterized by high signals for only the target analyte compared to other sample additives. Another im-

portant control experiment evaluates the device with non-imprinted polymers (NIPs). The resulting data typically reveals high MIP signals and low NIP signals. This literature review only discovered one research group that templates NIPs against an analog molecule to the template (39, 103). Otherwise, the field is dominated by reports that assess their technique with an NIP having no template. This laxity results in MIPs and NIPs with significantly different porosity, specific surface area, and pore volume, thus detracting from a rigorous persuasion of selectivity (104).

2.3. Biosensor Applications

MIPs are applied to a wide variety of biomedical applications. For example, graphene has been composited with MIPs to quantify dopamine (DA) in human serum and urine (105). Similarly, tryptophan has been measured in human serum with MIPs composited with carbon nanotubes (106). Lastly, cancer detection has been evaluated through a comparison of MIP-based optical and ECM biosensors (107). More examples are contained throughout this review.

MIP-based biosensors are also routinely developed for the

Table 3a. Summary of the case studies highlighted in this review and organized according to adopted nanomaterial.

NM	Advantages	Challenges	Case Studies			
			"Analyte [Reference]"	Sensitivity	"Sample Media"	Achievements
AgNMs	Low-cost, Adaptable plasmonics, High electrical conductivity	Potentially toxic	"Furfural [110]"	LOD = 0.03 ppm	Alcoholic & Caffeinated Bevarages	Novel, facile, & low-cost optical biosensor
			"Quercetin [122]"	0.02 - 250 µM	PB, Supplement tabs	Good sensitivity with an easily renewed, disposable electrode
			"Imidacloprid [111]"	0.200 - 800 ng mL^{-1}	Various vegetables	Multistage signal enhancement via Ag dendrite & AgNP layers separated by MIP layer
AuNMs	High electronic conductivity, Adaptable plasmonics; Molecular binding via thiol links	Reproducible SPR requires homogenization, Potentially toxic	"SA [127]"	0.0005 - 50 µmol L^{-1}	Water, wheat	ECM quantificaiton of SA via AuNP-MIP electrode modification
			"R6G [128]"	10^{-10} - 10^{-4} mol L^{-1}	Water, orange juice	Reproducible signal via AuNP array composited with MIP
			"NSE [129]"	0.0001 - 10 µg mL^{-1}	Serum	MIP binding to two separate analyte epitopes for selectivity & sensitivity increase
CNMs	Good electrical, mechanical, & optical properties	Surface modification required to mitigate toxicity (not C60); Poor water solubility	"DA CPZ [105]"	"0.05 - 8 µM, 8 - 40 µM; 0.005 - 2 µM"	PBS, supplement tabs, urine, human serum	Sensitive & specific parallel determination of DA & CPZ with graphene
			"Chlorambucil [137]"	1.47 - 247.20 ng mL^{-1}	Supplement tabs, urine, blood	Novel chlorambucil ECM detection with MIP and C60
			"Tryptophan [106]"	"0.002 - 0.2 µM, 0.2 - 10 µM, & 10 - 100 µM"	PBS, human serum	First tryptophan detection with MWCNTs & MIPs
MNPs	Facile fabrication & modification, Sample manipulation, Electrically conductive	Modificaiton required to promote safety or dispersal	"Cyfluthrin [108]"	10^{-8} - 10^{-3} mol L^{-1}	River water	Unique nanomaterial composition of Fe, GO, & AgNPs with MIP for SERS biodetection
			"CAP [112]"	0.5 - 50 ng mL^{-1}	PBS, fish, & pork	Small analyte (~ 323 g mol^{-1}) sandwich immunoassay
			"Cyfluthrin [152]"	30 – 3000 ng mL^{-1}	Honeysuckle	Analyte extraction
			"Diuron [59]"	0.1 - 10.0 mg L^{-1}	Water, methanol, grain-related samples	SiO2 coated IOMNPs for sample pre-treatment prior to HPLC analysis

assessment of environmental samples. River water samples were evaluated for the relative amount of the insecticide cyfluthrin by compositing MNPs with MIPs in an optical biosensor (108). Soil samples were tested for the herbicide diuron with a MIP-based HPLC strategy (59). Air streams have been monitored for the abundance of formaldehyde using a MIP-based gravimetric biosensor (109).

Similar to environmental monitoring, food safety is an important application for MIP-based biosensors. One such example involves furfural monitoring in alcoholic and caffeinated beverages by compositing nano silver with MIPs (110). Another example achieved the selective detection of the insecticide imidacloprid in vegetable samples (111). Lastly, an antibiotic has been quantified in samples of fish and pork by compositing MNPs with MIPs (112). While some of the case studies highlighted in this review deal with environmental and food safety, their strategies are amenable to biomedical analyte monitoring.

3. Nanomaterials

This review's definition of nanobiosensor, derived from the National Nanotechnology Initiative (NNI), is a sensor that quantifies a biological analyte and that also possesses some component which measures or functions on the nanoscale (113). Generally, biosensors investigators turn to nanomaterials to access high specific area to volume ratios that lead to higher sensitivity, but particular nanomaterials offer their own unique advantages (86, 114). However, nanomaterials present challenges like toxicity, agglomeration, and aggregation (87, 115, 116). Just as a given nanomaterial offers specific advantages to an application, particular nanomaterials present their own unique challenges (86, 87). A wide variety of nanomaterials are applied to MIP-based biosensors, but this review focuses on silver, gold, carbon, magnetic, quantum dot (QD), SiO_2, and TiO_2 nanomaterials. There are several ways to arrange nanomaterials with MIPs. For example, with core-shell morphology (Fig. 2a) some carrier NP with a MIP envelope contains the bound template and sometimes other nanomaterials. The template is removed after polymerization via elution leaving epitopes for the analyte (Fig. 2b) (95). Such a nanocomposite might be applied to a sandwich immunoassay (Fig. 2c). Other strategies deposit MIP thin layers onto cantilever or electrode substrates for selective analyte binding (Fig. 2d). The following systematically discusses select nanomaterials leveraged for MIP-based biorecognition in biosensors (Table 3).

3.1. Silver Nanomaterials (AgNMs)

As a nanomaterial, silver exhibits a wide array of useful attributes that lends it to many diverse biomedical applications (117-119). In this section, a discussion of compositing AgNMs with MIPs is presented. AgNMs alone contribute several benefits to biosensor applications, such as its low cost, adaptable plasmonic properties, and high electrical conductivity. For the most part AgNMs do not present significant or unique challenges to biosensing. However, like most nanomaterials, some attention must be paid to effective dispersal as well as toxicity. While the biosensors reviewed here are not intended for internal use, the component materials may still find their way into the environment or come into contact with the user. In that case, nano silver's environmental toxicity (120) and its potential to enter the body (121) cannot be discounted.

Silver nanoparticles (AgNPs) and MIPs have been combined in an optical biosensor to detect furfural, a carcinogenic and hepatotoxic flavor/aroma additive used in the food industry (110). Compared to a conventional surface plasmon resonance (SPR) biosensor, this work presents a facile strategy for quantifying analyte concentration changes. Researchers performed an analyte concentration study of intensity versus wavelength. A polychromatic light source was passed through a sample chamber containing linear AgNP-patterning achieved via controlled inkjet printing. For selective analyte binding a MIP layered onto the substrate within the sample chamber was prepared (Fig. 2d). The researchers report a LOD of 0.03 ppm for furfural in caffeinated and alcoholic samples. Although the results are encouraging, this report does not include a sensitivity range nor any selectivity control experiments such as assessment with NIPs or analogous compounds to furfural.

Another instance utilizing AgNPs takes advantage of their enhanced electrical conductivity to overcome a MIP's insulating nature. The reported ECM sensor also makes use of MNPs and reduced GO resulting in a nanocomposite modification to the electrode (122). The MIPs were arranged in a thin layer (Fig. 2d). Compared to other ECM sensors tabulated by the authors their device exhibits a better than average linear detection range from 20 nM to 250 μM and an LOD equal to 13 nM. Where it surpasses the competition is the fact that its electrode is disposable and quickly renewed via external magnetic field application. The linear detection range is determined in phosphate buffer (PB) and the strategy is further assessed by quantifying quercetin in dietary supplement tablets.

A compelling application of AgNMs involves the novel construction of a paper sample collector for enhanced and specific imidacloprid monitoring, a neonicotinoid insecticide (111). The device's chip is comprised of a paper substrate upon which dendritic silver was produced. These were layered with a molecularly imprinted membrane via electropolymerization (Fig. 2d). Additional AgNPs were decorated upon the molecularly imprinted membrane. This last step effected an increase in the signal. The authors reported a linear detection range from 0.200 to 800 ng mL^{-1}. The sensor is capable of quantifying imidacloprid in real samples prepared from vegetables and grains. It demonstrated stability by outputting consistent data from paper chips stored at varying temperatures. Selectivity was demonstrated in an assessment for the target pesticide when potentially interfering pesticides were present.

3.2. Gold Nanomaterials (AuNMs)

Like silver, AuNMs have long demonstrated their merit toward many biomedical applications (80, 123, 124). Regarding biosensors, AuNMs are valued for their capability to enhance ECM and optical transduction strategies. It follows that MIP-based

biosensors also benefit from incorporating AuNMs (125). The major disadvantages associated with AuNMs, namely dispersibility and toxicity, are manageable. Many conventional biosensors employ AuNMs for antibody binding, taking advantage of thiol linkages (79, 126). Having eliminated those unreliable and expensive binding strategies, MIP biosensors often still make use of AuNMs. Here, several state-of-the-art biosensors reports are highlighted, which combine AuNMs for sensitivity enhancement with MIPs for selectivity.

First, researchers describe an ECM strategy leveraging AuNPs for their high electronic conductivity to increase the sensitivity of the biosensor (127). This research provides a rare report of salicylic acid (SA) detection in plant matter, which is critical for accurately determining the phenomena governing the defense, development, and growth of grains. The strategy boasts a sensitivity range from 0.0005 μmol L^{-1} to 50 μmol L^{-1}. The strategy was demonstrated in real biological samples by quantifying SA added to wheat. MIPs generated more signal than the control NIPs. These MIPs were layered onto an electrode via precipitation polymerization in acetonitrile for selective SA binding (Fig. 2d).

In another recent compositing of AuNMs with MIPs, rhodamine 6G (R6G), a toxic fluorescent dye not yet banned from food stuffs in some countries, is quantified (128). An array of gold nanoparticles (AuNPs) achieves a homogeneous arrangement of "hot spots" resulting in increased surface enhanced Raman spectroscopy (SERS) signal reproducibility. A porous MIP achieves improved mass transfer enabling the target molecule to interact with the hot spots. Figure 2(d) depicts this MIP conformation. The sensor exhibits linear sensitivity between 10^{-10} to 10^{-4} mol L^{-1} in deionized water. It was also selective for the analyte in orange juice. Moreover, it was effective for R6G sensing even in the presence of the following chemical analogs: rhodamine 123, crystal violet, and rhodamine B.

One final combined use of MIPs and AuNMs investigates the application of SERS sensing for protein disease markers like neuron-specific enolase (NSE) (129). This is a particularly impactful contribution to the field as it directly attacks the well-known problem of detecting proteins with MIPs (100, 130). MIPs were employed for the dual purposes of analyte isolation and labeling. This is achieved by preparing two specific MIPs for two corresponding epitopes on the same target protein. A layer of AuNPs and MIP for one epitope is oriented on a substrate for analyte capture. Then AgNPs, composited with MIP for a different epitope, are added to the sample for analyte labelling. The described configuration is comparable to Fig. 2c, where one MIPNP contains silver in its core and the other MIPNP is replaced with a MIP layered onto a gold substrate. This sandwich immunoassay strategy, along with the synergistic effects of Au and Ag, result in a highly selective and sensitive sensor. The strategy demonstrated a linear detection range in standard samples from 100 pg mL^{-1} to 10 μg mL^{-1}. For comparison purposes enzyme-linked immunosorbent assay (ELISA) calibration was also determined with real human serum samples, but the conventional technique yielded a significantly narrower sensitivity range. ELISA took 6 times longer to complete, included more than double the number of steps, and required 20 times the sample volume. The report also included checks for selectivity by assessing analogs to NSE like bovine serum albumin (BSA), horseradish peroxidase, ribonuclease A, and ribonuclease B with no more than 7% cross-reactivity. Evaluation of NSE in healthy patient human serum and small cell lung cancer patient human serum demonstrates the strategy's potential to real world applications.

3.3. Carbon Nanomaterials (CNMs)

CNMs are varied in their conformations, such as sheets of graphene oxide (GO), fullerenes, carbon nanotubes, and more. They manifest several beneficial properties making them desirable for diverse biomedical applications (131-134). Aside from biosensors, recent reports indicate the potential for composites of GO with MIPs for drug delivery (135, 136). CNMs are employed to take advantage of electrical, mechanical, or optical properties.

An interesting work that combines the advantages of MIPs and GO succeeds in quantifying both dopamine (DA) and chlorpromazine (CPZ) at the same time (105). This is achieved through electropolymerization of MIPs in the presence of both analytes. The study achieves enhanced ECM signal via employment of QDs comprised of GO and doped with nitrogen. These optimize the electroactive region on the sensor's surface and improve the rate of charge transfer. Two linear detection ranges for DA were found: the first from 0.05 to 8 μM and the second from 8 to 40 μM. For CPZ, the linear detection range was from 0.005 to 2 μM. These ranges are either more sensitive or wider than other recent and comparable efforts to quantify these analytes. Other efforts are not capable of assessing both DA and CPZ simultaneously. The report demonstrates amenability to real world applications by assessing both analytes in media like pharmaceutical samples, urine, and human serum. Evaluation of this ECM sensor proved selective when potentially interfering substances were present, like glucose, urea, creatine, and others.

Another innovative compositing of CNMs with MIPs is presented, wherein the researchers report the first chlorambucil detection via MIP binding (137). Insulating chlorambucil imprinted micelles were composited with water insoluble carbon 60 to realize ECM detection of the cancer fighting compound. The analyte's linear detection range was between 1.47 and 247.20 ng mL^{-1} for aqueous samples. The sensor was capable of reliably detecting the analyte in pharmaceutics, urine, and blood plasma. The strategy was reliable in the presence of interferents like other cancer fighting compounds (i.e. melphalan, 5-flurouracil, and temozolomide) as well as some biologically relevant compounds (i.e. DA, uric acid, and glucose).

Multi-walled carbon nanotubes (MWCNTs) have been layered onto an ECM sensor electrode with inexpensive, biocompatible chitosan MIPs for determination of tryptophan (106) (Fig. 2d). The MWCNTs nullify the MIP's natural inhibition of the electrode's conductivity. The strategy was capable of de-

tecting tryptophan in PBS in three linear ranges: 2.0 nM to 0.2 μM, 0.2 to 10 μM, and 10 to 100 μM. Commonly encountered interferents like tyrosine, uric acid, DA, and ascorbic acid are inconsequential. A real sample of human serum was assessed with good results.

3.4. Magnetic Nanoparticles (MNPs)

Of all the fields of study using MNPs, biomedical applications are the most prevalent and encouraging (138-140). Besides nanobiosensors, they have demonstrated an efficacy toward hyperthermia cancer treatment, imaging contrast, drug delivery, as well as cell, nucleic acid, or protein isolation (141-143). MNPs coupled with conventional binding strategies (e.g. antibodies) (144, 145), allow for various magnetic transduction strategies like giant magnetoresistance (GMR), Hall effect, superconducting quantum interference device (SQUID), etc. (29, 146-150). Unfortunately, no reports (Fig. 1) describe MIP binding coupled with magnetic transduction; none could be found at the time of writing and this omission is acknowledged elsewhere (43). While there exists a paucity of reports on true magnetic biosensors utilizing MIPs for analyte binding, there are many MIP reports that leverage MNPs for sample heterogenization, thereby enhancing analyte concentration (99, 151).

SERS biodetection is advanced through a nanocomposite comprised of an MNP core for sample purification as well as GO layer and AgNPs for signal enhancement (108). This nanocomposite was further functionalized with an MIP via precipitation polymerization of the functional monomer acrylamide within the shell of the construct (Fig. 2b). SERS enables non-destructive sample processing, favorable sensitivity, and rapid operation. The method detects the insecticide cyfluthrin in river water samples from 10^{-8} to 10^{-3} mol L^{-1} with good linearity. The technique is specific only for the target analyte when compared against the chemically similar compounds bifenthrin and fenvalerate. The Raman signal intensity was more than two times stronger for the target analyte when compared to the analogs.

A separate report also uses MNPs and MIPs to detect cyfluthrin. Again, MNPs in this work only serve to realize analyte purification (152). MIP functionalized MNPs efficiently extract the pesticide cyfluthrin from honeysuckle samples. The conformation of this nanocomposite is similar to Fig. 2b. Rather than quantify cyfluthrin using a novel nanobiosensor, conventional high performance liquid chromatography (HPLC) is employed. Linear sensitivity is demonstrated from 30 to 3000 ng mL^{-1}. The researchers demonstrate their selectivity toward cyfluthrin through a binding investigation of MIP and NIP performance compared to other insecticides.

The next investigation realizes detection of the antibiotic chloramphenicol (CAP) in food with a sandwich assay and personal glucose meter (PGM) quantification (112). CAP de-

Table 3b. Summary of the case studies highlighted in this review and organized according to adopted nanomaterial.

NM	Advantages	Challenges	Case Studies			
			"Analyte [Reference]"	Sensitivity	"Sample Media"	Achievements
QDs	Dispersibility & fluorescent properties	Toxic conventional fabrication (e.g. CdSe) due to heavy metal content	"SCCA [164]"	0.0001 - 100 ng mL^{-1}	PBS, human serum	Sensor surface protection from transducing species via Fe-based MOF co-reaction accelerator
			"MA [165]"	5.0 - 250 μM	PBS, urine, plasma	Proximate orientation of eco-friendly CQDs & MIPs for high mass transfer
SNMs	Biocompatible, Facile silanization modification, Amenable to periodic porosity, High surface area, Tunable pore size, Chemically stable	Irregular porosity & short crosslink distances leads to insignificant swelling	"Serotonin [171]"	0.01 - 1000 μM	Supplement tabs, urine, PBS	Unique realization of AKD-PAD for serotonin detection with MIPNPs
			"pTyr [172]"	0.07 – 230 μM	PBS, β-casein tryptic digest	Microwave fabrication of SiO2, QD, & MIP nanocomposite
			"Sparfloxacin [173]"	0.05 – 2.0 μg mL^{-1}	PBS, human serum	One-pot, thiol-ene click compositing of MSN & MIP
TNMs	Good catalysis & electron transfer, Biocompatible, High surface area, Chemically stable	No intrinsic selectivity unlike SNMs	"Toltrazuril [177]"	0.43 - 24.54 μg L^{-1}	Chicken muscle, egg	Intelligent NM selection for sensitive & selective detection
			"p-NP [178]"	0.01 - 80 μmol L^{-1}	PBS, milk	Facile ECM p-nonylphenol detection from food media
			"Bilirubin [179]"	0.01 - 120 μM	PS, serum	Surface area enhanced red mud carrier for surface MIP QCM bilirubin biosensor

tection was possible in the presence of interferents like tetracycline, streptomycin, and oxytetracycline. The strategy boasts of an LOD of 0.16 ng mL^{-1} and a detection range from 0.5 ng mL-1 to 50 ng mL^{-1}. The combination of PGM and MIPs contribute to fast, portable, facile, inexpensive, reusable, and stable implementation. These benefits can be attributed to the PGM's half century of optimization (153) and MIP substitution of antibodies as target analyte binding strategy. These MIPs were created from fragment imprinting where only part of the target is contained within the polymer leaving other parts exposed to other binding sites. AuNPs were used to adhere invertase to β-cyclodextrin, which was used due to its unique attributes. β-cyclodextrin couples with nitrobenzene through its hydrophobic cavity. EnVision polymeric chain was used to load many invertase tags. Hydrolysis of sucrose to glucose through invertase action amplified the signal for PGM readout. The m-MIP allowed for magnetic washing upon analyte binding. The analyte was also captured by the invertase entity for tagging. The described sandwich immunoassay is comparable to Fig. 2c, but with one NP replaced by the β-cyclodextrin-invertase tag.

Another report describes silica-coated MNPs for surface polymerization imprinting (Fig. 2b). Silica ameliorates agglomeration and paves the way for surface polymerization imprinting with methacrylic acid (MAA) as functional monomer (59). Diuron, a known water contaminant, spiked into water and methanol was assessed with HPLC. The method obviates conventional, and time-intensive, sample pre-treatment. This strategy resulted in a linear sensitivity for diuron from 0.1 mg L^{-1} to 10.0 mg L^{-1} and an LOD equal to 0.012 mg L^{-1}. The authors demonstrated selectivity for diuron by detecting the target in paddy water, paddy soil, and grain seedlings also spiked with chemically similar analogs (fluometuron, chlorotoluron, and isoproturon) in addition to several reference compounds (altrazine and terbutylazine).

Besides sample manipulation, some strategies take advantage of an increased electrical conductivity native to iron oxide MNPs. Also, MNPs can be produced and functionalized in a facile manner to be biocompatible and dispersible in any medium. However, MNPs have much more to offer. Since biological samples exhibit negligible magnetism, magnetic transduction with MNPs suffers from little background signal resulting in high sensitivity (154, 155). Therefore, it is expected that magnetic transduction researchers will soon realize the potential in abandoning conventional analyte binding (e.g. antibodies) in favor of a MIPs. Consider that an MNP's magnetic susceptibility, or the extent of magnetization versus applied magnetic field, can be correlated with the amount of analyte bound to a surrounding MIP layer (142). In that case, magnetic transduction strategies relying on magnetic relaxation, like SQUID (156, 157) or Fluxgate biosensors (158, 159), are expected to perform well with MIPs. Similarly, MIP functionalized MNPs should be amenable to a variety of magnetoresistance transduction strategies like GMR (160, 161). Figure 3(a) is a depiction of a magnetoresistance transducer employing an MIP, for selectivity, layered on an MNP, for signal generation dependent on the amount of bound target analyte.

3.5. Quantum Dots (QDs)

Quantum dots are also leveraged to advance fluorescence and luminescence devices (162, 163). The virtue of QDs has been demonstrated by their propensity to avoid photobleaching, size-dependent light emission, enhanced brightness, relatively large absorption coefficient, and tight emission spectrum. Conventionally, QDs were toxic detracting from their application in biomedicine. However, advances in fabrication have mitigated toxicity and improved solubility by realizing production in water. Furthermore, some of these can be made not to contain heavy metals.

An interesting incorporation of QDs comprised of zinc selenide, or ZnSeQDs, into an iron-based metal organic framework (MOF) was reported for the determination of squamous cell carcinoma antigen (SCCA) in human serum (164). The report details the realization of biosensor interface protection from the peroxydisulfate transducing species. The fabricated MIP thin layer is comprised of polydopamine for biocompatibility and amenability to tailored absorption. This is possible with the MOF acting as accelerator of the co-reaction with ZnSeQDs. These luminophores were selected for their excellent luminescence and relevance to similar analyte detection, namely carcinoembryonic antigen (CEA). Sensitivity in PBS from 0.0001 to 100 ng mL^{-1} was demonstrated with an LOD equal to 31 fg mL^{-1}. The electrode was recyclable up to five times and the electrochemiluminescence (ECL) strategy was specific to SCCA when interferants like CEA, BSA, α-fetoprotein, and cancer antigen 153 (CA-153) were present. NIP formulations exhibited a negligible signal.

Mandani et al. report a state-of-the-art utilization of QDs for fluorescent probe labels in determination of methamphetamine (MA) (165). The report details the facile coating of eco-friendly carbon QDs (CQDs) onto a core-shell mesoporous silica nanoparticle (MSN) with MIP layer coinciding with CQD layer. The described configuration is like Fig. 2b, except that CQDs are in proximity to the MIP binding sites. This sol-gel fabrication, which realizes proximate positioning of fluorescent label with MIP recognition, allows for increased analyte binding and easier removal due to improved mass transfer. Linear detection ranges from 5.0 to 250 μM with an LOD equal to 1.6 μM as measured in PBS. The device was reusable up to five times without the need for refreshment. MA selectivity was demonstrated in the presence of interferants like ascorbic acid, uric acid, glycine, alanine, DA, caffeine, and morphine. Also, ions like K^+, Ca^{2+}, and Cl^- were allowed to interfere with negligible impact. Selectivity was further demonstrated by the fact that NIPs exhibited significantly lower fluorescence compared to MIPs. This strategy demonstrated its potential toward real world applications in biological samples such as human urine and blood plasma.

3.6. Silica Nanomaterials (SNMs)

Many MIP-based nanobiosensors adopt silica as the functional

monomer matrix for containing selective binding sites for the target analyte (166, 167). Silica readily adapts itself to this application as a result of its biocompatibility, facile functionalization through silanization, potential for periodic porosity, high surface area to volume ratio, tunable pore size, and chemical stability. These attributes also make SNMs suitable for drug delivery applications (168-170). The challenges in working with silica-based MIPs are in mitigating irregular porosity and short crosslink distances. These lead to insignificant swelling, meaning special care is required to precisely manipulate crosslinking density and related mass transfer.

The authors of a recent investigation report efforts to enhance electrical conductivity of MIP binding in an ECM serotonin biosensor (171). Nanocomposites prepared in this study were of the core-shell variety (Fig. 2b). The MIP shell was comprised of serotonin-specific binding sites embedded in a silica layer. Within the core, they employ magnetite and gold nanocomposites for improved electrical conductivity. Besides improving the rate of electron transfer, the magnetite MNPs enable magnetic washing. The ECM biosensor detects serotonin with an LOD of 0.002 μM and boasts a linear detection range from 0.01 to 1000 μM. Serotonin detection was achieved in solutions derived from either over-the-counter pharmaceutical products or human urine. Selectivity was assessed with NIPs, interferants, and structural analogs, like magnesium sulfate and creatinine.
Another recent contribution to the use of silica as MIP for biosensor applications details their novel fabrication via microwave-enabled synthesis (172). This heating method, rather than hydrothermal synthesis, is credited with the rapid manifestation of monodisperse and controlled nanomaterial. The authors attribute this to the higher quantum yield, which relates to the strategy's improved selectivity and sensitivity. The core-shell nanocomposite (Fig. 2b), employs a mesoporous silica layer for adherence to the QD core, inherent biocompatibility, and regular porosity. The cadmium telluride QDs enable optical fluorescence determination of tyrosine phosphopeptide (pTyr). This strategy demonstrates a linear detection range between 0.07 and 230 μM as well as an LOD equal to 34 nM. The potential application toward real sample evaluation was demonstrated in solutions comprised primarily of β-casein tryptic digest spiked with pTyr. Selectivity was addressed by investigation of several interferants including multiple ions, ascorbic acid, uric acid, fructose, glucose, various proteins, and some peptides chemically similar to pTyr. The device's detection signal with NIPs was significantly diminished as compared with MIPs.

One final contribution to the adoption of mesoporous silica for molecularly imprinted materials utilizes thiol-ene click chemistry to realize a novel functional monomer (173). The one-pot formulation realizes custom binding sites on the favorable specific surface area of mesoporous silica. The strategy exhibits linear sensitivity in PBS and human serum for sparfloxacin from 0.05 to 2.0 μg mL^{-1} and an LOD equal to 0.012 μg mL^{-1}. The mechanism of operation is optical fluorescence made possible with zinc sulfide QDs doped with manganese. Selectivity was demonstrated by comparing the performance of the strategy with the chemically similar compounds gatifloxacin, ciprofloxacin (CPX), clindamycin, and norfloxacin.

3.7. Titanium Dioxide Nanomaterials (TNMs)

TNMs often serve as support upon which other nanomaterials are assembled. Additionally, TNMs possess distinctive properties making them appropriate for certain MIP biosensors strategies. They exhibit good catalytic activity and electron transfer, are biocompatible, have a large surface area to volume ratio, and are chemically stable. Also, TNMs are inexpensive and exhibit good optical properties. For these reasons, there are many relevant investigations into TNMs applied to biosensors using MIP binding, as discussed in this section (174-176). The most significant challenge associated with TNMs, unlike SNMs, is that they possess no intrinsic analyte binding affinity.

To begin, researchers describe a successful ECM biosensor for point-of-use testing of toltrazuril contamination in animal food products (177). The device benefited from an MIP-layered electrode (Fig. 2d), for selective template binding. The MIP reported here is synthesized from beta-cyclodextrin as monomer for host-guest interaction between the template and monomer, thus realizing non-covalent binding. TiO_2 enhances the conductivity of the platinum substrate for increased sensitivity. The researchers demonstrate linear detection from 0.43 to 42.54 μg L^{-1} using differential pulse voltammetry more sensitively than both UPLC and LC-MS/MS. However, the sensor cannot detect the template at higher concentrations, meaning that conventional detection is not wholly replaced. Not only does the MIP exhibit obvious template affinity as compared to NIP performance, but the biosensor is not subject to interferants like glucose and ions like sodium or potassium.

A recent incorporation of TiO_2 nanoparticles and MIPs in an ECM biosensor realizes facile implementation of p-NP quantification in food samples (178). MIPs were layered on a glassy carbon electrode (Fig. 2d) for selective analyte binding. The strategy exhibited a linear sensitivity between 0.01 and 80 μmol L^{-1}, as well as an LOD equal to 3.91 nmol L^{-1} as measured in spiked samples of isopropanol and PBS. Target selectivity was evident upon significantly reduced ECM signal generated from the chemically similar compounds 4-aminophenol, phenol, bisphenol A, 4-bromophenol, and 4-octylphenol. Application to real samples was demonstrated with solutions containing milk powder. The sensor was stable after as many as four weeks.

One unusual case study, departing from both ECM and optical biosensor transduction, makes use of TiO_2 nanoparticles for the enhancement of surface area. Investigators report a surface imprinting of polypyrrole onto colloidal red mud (179). Besides enhancing surface area, red mud, comprised of Al2O3, SiO_2, Fe_2O_3, and TiO_2, also leverages good adsorption and mechanical attributes, despite no innate recognition capability. The template was bilirubin, for which the sensor exhibited linear sensitivity between 0.01 and 120 μM and an LOD equal to 0.003 μM in PBS. This gravimetric biosensor employed a quartz crystal microbalance for mass determination, meaning

Table 4. Summary of the case studies highlighted in this review and organized according to the adopted nanobiosensor transduction strategy.

Transduction Strategy	Advantages	Challenges	Case Studies			
			"Analyte [Reference]"	Sensitivity	Sample Media	Achievements
Optical	High & wide sensitivity, Low LOD, Facile & low-cost assembly, Non-destructive	Labels required for maximal sensitivity	"BHb [188]"	LOD = 0.911 μg mL^{-1}	PBS	"No surfactants; Macromolecule recognition"
			"Tramadol [189]"	0.0030 - 2.5 μM	PBS, urine, serum	Spatially close oxidized & non-oxidized species promote energy transfer & stability
			"CA-125 [107]"	"ECM: 0.01 - 500 U mL^{-1} SPR: 0.1 - 300 U mL^{-1}"	PBS, artificial serum	Direct comparison of ECM vs Optical techniques both using MIPs
ECM	"Miniaturizable, Low-cost, Sensitive, Specific ECL targets non-electroactive analytes reducing interference"	"MIPs inhibit conductivity, Macromolecules adhere to electrodes, Limited sensitivity, Poor LOD ECL wearable strategies are not continuous since device refreshment is required"	"cTnI [196]"	0.01 - 5.00 ng mL^{-1}	PBS, plasma	Low LOD vs earlier ECM strategies, enhanced performance via sandwich assay
			"Cocaine [103]"	1 nM - 1 mM	PBS, plasma	Compelling selectivity demo via NIP templating to cocaine analog
			"Lactate Urea [197]"	"0.050 - 1.0 mM, 2.5 - 20.0 mM; 0.045 - 19.5 mM"	PBS, methanol, artificial & human sweat	Wearable, ECL sensor with selective MIP layer
			"DA [198]"	10^{-14} - 10^{-6} M	"PBS, rat serum"	Enhanced upconversion NPs & MIP embedded AuNPs for synergistic ECL detection
Gravimetric	Fast, Sensitive, Inexpensive, Facile assembly, Selective, Label-free, Air or liquid operation	Sample homogenization, Inefficient transduction integration, Low response time upon miniturization, Poor multiplexing capability	"CPX [204]"	1.5 - 150.9 μM	Water	Sensitive, dry operation
			"TCF [205]"	0 - 250 ppb	Water, iceberg lettuce	Simplified fabrication avoiding in situ polymerization
			"PSMA [206]"	0.01 - 100 ng mL^{-1}	PBS, mouse serum	Hydrophilic MIP hybridized with Love SAW sensor
			"DLP [207]"	indeterminate	Acetonitrile	Functionalization during harsh photolithography fabrication & vacuum operation

the MIP was layered onto a substrate (Fig. 2d). The device exhibited reproducibility by way of about 3% performance loss after 20 uses and about 4% loss after 5 months post-fabrication. Selectivity was established with good serum sample performance and minimal response to the chemical analogs cholesterol, testosterone, and biliverdin as well as minimal response to the prepared NIP formulation.

4. Nanobiosensor Transduction Strategies

There is a wide variety of strategies for converting the binding event of some target bioanalyte and a MIP into an electronic signal for output, including ECM, optical, gravimetric, magnetic, and thermometric (21-23, 180). In the above MNP section, this review draws attention to the fact that while magnetic transduction and MIPs appear compatible, there are no case studies to present. Presumably, magnetics experts will soon apply m-MIPs to magnetoresistance transduction (Fig. 3a) or to magnetic transduction relying upon MNP relaxation times (29,

181, 182). Similarly, thermometric transduction lies outside the scope of this review. Instead, the following discussion presents several state-of-the-art optical, ECM, and gravimetric transduction strategies for nanobiosensors. The following systematically discusses select transduction strategies leveraged for MIP-based biorecognition in biosensors (Figure 3 and Table 4).

4.1. Optical Transduction

While optical transduction strategies employing MIPs for nanobiosensors are not as prominent in the literature, they are a close second to ECM strategies. Of the reports reviewed here (Tables 3 and 4) nearly 31% of them are optical by design (Fig. 1d). These strategies can be further subcategorized into biosensors employing optical resonators, SPR, optical fibers, optical waveguides, photonic crystals, and others. The advantages associated with optical transduction are numerous (183-185). They can be miniaturized, are reliable in that their operation is not susceptible to the environment, and are renowned for their sensitivity. Optical biosensors are capable of facile sample handling like minimal pretreatment and the non-destructive nature of biosensor operation on the sample (27). When nanomaterials are incorporated into optical biosensor design the product is improved. Several researchers are reporting the use of nanoparticles tagged to bioanalyte molecules to improve sensitivity (Fig. 3b). However, this solution requires the binding of a target analyte to a label, which is generally undesirable since it complicates sample processing and detracts from POCT (186, 187).

One report details the employment of casein protein-facilitated emulsion synthesis of surface MIPs for bovine hemoglobin (BHb) biosensing (188). The authors reason that Pickering emulsion is wanted since it enables surface imprinting. By using the casein nanoparticle as stabilizer, the process is safer and less expensive by excluding traditional chemical surfactants. The authors address the difficulties with imprinting for relatively large macromolecules. Protein template removal is

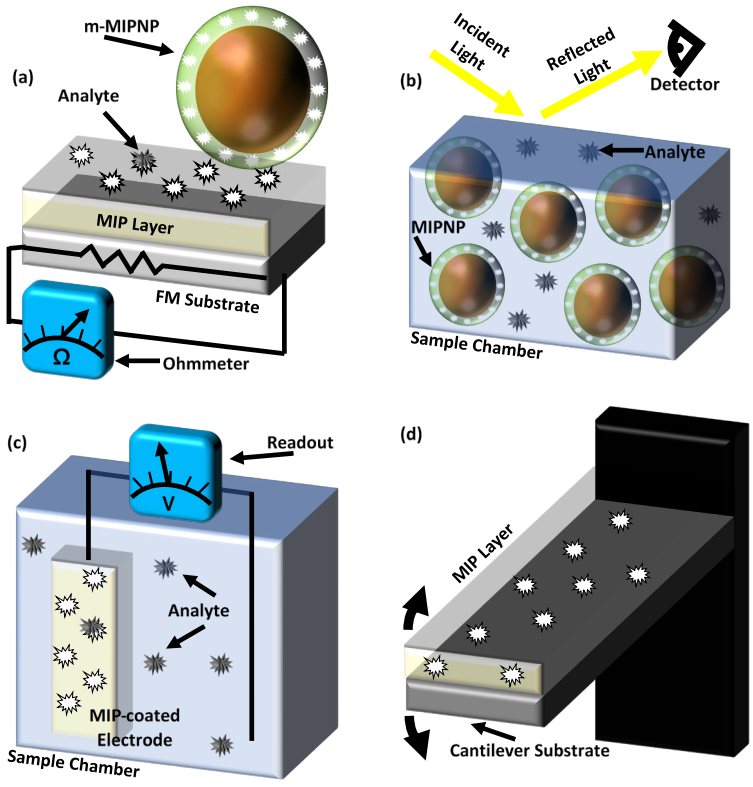

Figure 3. (a) A near-future magnetic transduction strategy can deposit a nano-thin MIP layer onto a ferromagnetic substrate for magnetoresistance sensor operation. **(b)** Many optical transduction strategies monitor changes in light after it interacts with aqueous MIPNPs bound to analyte. **(c)** In some ECM transduction strategies, nano-thin MIPs are layered onto electrodes. **(d)** Some gravimetric transduction strategies monitor the characteristic frequency of an oscillating cantilever to determine the analyte's concentration.

problematic due to size and potential denaturation associated with harsh polymerization conditions (i.e. pH, temperature, solvent). By employing the casein nanoparticle Pickering emulsion, surface-based imprinting is achieved so that the diffusion of the analyte into the polymeric matrix is inconsequential. In order to demonstrate selectivity, the control target proteins include BSA, lysozyme, and trypsin. The reported LOD is 0.911 μg mL^{-1}. This work employs ultraviolet and visible spectroscopic characterization of samples to assess BHb concentrations dispersed in PBS.

In a separate investigation of surface imprinting, the authors describe a detection system for tramadol comprised of magnetite for sample manipulation, silicon dioxide envelope for further functionalization, and MIP envelope for specific tramadol selectivity (189). With this first nanocomposite the tramadol can be purified from a sample (urine or plasma) and detected via chemiluminescence (CL). This CL reaction was realized thorough reaction of R6G with potassium permanganate. The initially weak CL reaction was enhanced via copper nanoclusters (CuNCs) (15 x) and even more so with the inclusion of copper metal organic framework (CuNCs@CuMOF) (48 x). Extracted tramadol further enhanced CL in proportion to the analyte's concentration. Linear detection ranged from 0.0030 to 2.5 μM and an LOD of 0.80 nM was reported. The system did not suffer from interference with natural biological compounds nor from other drugs. NIPs were also evaluated with tramadol samples to demonstrate selectivity with good results. While the sensitivities reported here are impressive, the described analyte labelling involves magnetic sample washing for purification purposes, which complicates the process for prospective non-technical users.

A valuable report was published recently in which the authors disclose the comparison of an ECM biosensor with an optical biosensor, namely SPR, both of which were functionalized with MIPs(107). The fabrication of the sensors followed similar designs. Both sensor chips were constructed via analyte templating during the polymerization of pyrrole realized by cyclic voltammetry. Each sensor was used to quantify samples of PBS containing varying concentrations of cancer antigen 125 (CA-125). The ECM sensor exhibited a linear sensitivity ranging from 0.01 to 500 U mL^{-1}, while the SPR sensor's sensitivity was between 0.1 to 300 U mL^{-1}. It was found that the adsorption capacity of the ECM sensor was an order of magnitude greater than the SPR sensor. The improved performance of the ECM technique was explained in terms of the inconsistencies in surface roughness in the Au-layer between the film used in the ECM technique versus disk in the SPR technique. The authors also explain that in the ECM technique, analyte molecules far from the electrode can be detected, but in the SPR technique the target must permeate the polymer layer so as to be adsorbed onto the electrode. While the work is valuable as a comparison of ECM transduction to the SPR strategy, it does raise the question of how other optical sensor strategies would compare. Of course, this may necessitate the use of a label, like QDs or AuNPs, that was otherwise avoided throughout the report.

4.2. Electrochemical (ECM) Transduction

Historically, ECM transduction has been the most prominent biosensor operational mechanism. Nearly 38% (Fig. 1d) of the devices reviewed in this work (Tables 3 and 4) utilize ECM transduction, a clear majority. Consider the success of the PGM as an example of this fact (153, 190-192). ECM nanobiosensors are those that quantify a bioanalyte via measurement of an electrical signal occurring after recognition of that target with an MIP. A particular device's monitored signal subcategorizes ECM biosensors into those that rely on conductometry, potentiometry, impedance, and amperometry. The ECM strategy (Fig. 3c) benefits from a wide variety of benefits. Such devices are easy to miniaturize, inexpensive, selective, sensitive, capable of multiplex sensing, and easy to assemble (25, 180, 193). However, when MIPs are applied to ECM transduction strategies a fundamental handicap becomes apparent. The insulating nature of most functional monomers causes MIPs to inhibit ECM signal generation (167, 171, 194, 195), thus sacrificing sensitivity. Molecularly imprinted electrodes have been shown to suffer from the adhesion of large, dynamic molecules, like enzymes. An ECM device lacking the benefit of MIPs or other nanomaterials may suffer from prohibitive linear detection range, unacceptable selectivity, and poor LOD (106).

First, investigators report on a novel ECM sensor that quantitates cardiac troponin I (cTnI) (196). It achieves this through surface-based analyte detection onto an electrode comprised of an MIP embedded with boron nitride QDs, which lies on a glassy carbon electrode similar to Figs. 2(d) or 3(c). Compared to others this strategy is cost-effective, less wasteful, eco-friendly, and more efficient. The authors address reuse considerations; the sensor can be washed and reused less than 25 times. Regarding the fabrication of the nanobiosensor, QDs were made first. Then, pyrrole containing the target analyte was prepared in a voltammetric cell. The sensor was not sensitive to non-targets including myoglobin, BSA, and cardiac troponin T. It was sensitive to the target, cTnI, in the linear range from 0.01 to 5.00 ng mL-1 with an LOD equal to 0.0005 ng mL^{-1}. Samples were dispersed in PBS for calibration and in plasma (serum) for selectivity demonstration.

The next ECM case study details a new application of MIPs for cocaine quantification using a potentiometric device (103). MIPNPs were synthesized via solid-phase imprinting technique. The authors narrowed the choices of functional monomers through computational modeling of target analyte and monomer interactions. The three functional monomers with the highest binding affinity toward cocaine were progressed to an experiment optimizing their relative composition with respect to each other. Photopolymerization in organic solvent yielded nearly 20 times more MIPNPs and about 60 times faster compared to chemical polymerization in water. When detecting cocaine in PBS the sensor exhibited a sensitivity between 1 nM to 1 mM. Besides PBS, the nanobiosensor demonstrated selectivity by detecting cocaine in human serum. This research

group distinguishes itself in selectivity demonstration by employing NIPs that are actually templated against a non-target molecule, thus ensuring a compelling control experiment. The sensor's response corresponded directly to cocaine or benzoylecgonine concentrations and was insensitive to the control, galantamine. Since cocaine presented no functional groups for the purposes of templating the MIPs against, the researchers used benzoylecgonine for templating.

A biosensor was recently reported that boasts a wearable device for monitoring sweat via ECL transduction. The design adopts ingenious adhesion of luminescent ruthenium composite nanoparticles on a polymer and gold nanotube substrate for flexibility as well as MIP layer coating for recognition (197). This solution differs from the conventional ECM strategy in that it does not suffer from the same challenges with large target molecule (i.e. enzyme) adhesion to electrodes or the fact that the target need not be electroactive. The researchers demonstrate linear sensitivities for lactate between 50 μM and 1.0 mM as well as between 2.5 mM and 20.0 mM. In addition, linear detection of urea was possible between 45 μM and 19.5 mM. Detection was carried out in PBS, methanol, artificial sweat, and human sweat. Unfortunately, the device was not capable of continuous monitoring due to a need for refreshment via elution.

Another case study in ECL transduction utilized AuNPs embedded in an organic matrix as well as upconversion nanoparticles to achieve synergistic effects with MIP detection (198). AuNPs were chosen in this work for their superior surface area to volume ratio as well as their beneficial electrical conductivity. The AuNPs were embedded in a matrix of crosslinking oligoaniline to achieve electrical transmission in three dimensions, since the spacing between AuNPs is spanned by the organic material, regardless of where a recognition site might be located. This MIP matrix was polymerized from the functional monomer aminothiophenol. A biocompatible, lanthanide-doped nanoparticle was used to produce optical light upon near-infrared laser irradiation. The operation of this upconversion nanoparticle was intensified via employment of covalent organic framework for its constant porosity as well as favorable selective recognition, surface area, stability, and density. These different nanomaterials obviated the usual disadvantage of poor MIP conductivity and resulted in a highly sensitive and specific device. This ECL sensor detects DA in the linear range from 10^{-14} M to 10^{-6} M with an LOD equal to 2 x 10^{-15} M in PBS. The device proved capable of distinguishing DA from chemically similar compounds like caffeic acid, adrenaline, and α-phenylethylamine, as well as the interfering compounds ascorbic acid and uric acid. When all these compounds were present in rat serum DA elicited a signal approximately three times stronger than any of the others.

4.3. Gravimetric Transduction

Gravimetric nanobiosensors take advantage of the unique mass of the target analyte to achieve selectivity. Examples of this strategy include the piezoelectric cantilever, the quartz crystal microbalance (QCM), mirco electromechanical systems (MEMS), and surface acoustic wave (SAW) devices (199-202). In general, gravimetric biosensors benefit from many attributes: fast to yield results, sensitive to analyte concentration, inexpensive to construct, and selective for the intended targets. The strategy enjoys facile sample handling due to the label-free operation which can occur in air or liquid. However, gravimetric biosensors attract less attention from researchers compared to other strategies. Only about 13% of the papers reviewed in this work (Tables 3 and 4) utilize gravimetric transduction (Fig. 1d). This is despite the fact that gravimetric nanobiosensors exhibit comparable performance versus ECM devices (203). Unfortunately, since the analyte must come into direct contact with the transducing surface, sample homogenization is required which can add time or steps to the process.

Gravimetric biosensors are experiencing renewed interest due to the potential of MIPs to eliminate wet operation required by antibodies for analyte binding. MIPNPs have been functionalized onto a microcantilever for sensitive mass detection of analyte (204). Investigators describe the preparation of MIPNPs with double phase emulsion polymerization. Specific binding is possible via templated cavities wherein the carboxyl groups of the functional monomer, MAA, noncovalently attracted certain parts of the target analyte. MIPNPs were decorated onto a microcantilever and dynamic sensing mode detected resonant frequency changes after analyte binding. The sensor exhibited a linear detection range for CPX between 1.5 and 150.9 μM. Sensor selectivity for CPX was demonstrated through negligible frequency changes during NIP functionalized microcantilever experiments as well as separate interferent enrofloxacin detection. This strategy is facile, inexpensive, and time efficient compared to conventional nano electromechanical systems (NEMS).

Investigators recently described a unique sensor fabrication obviating the tedium of polymerization (205). This is achieved with commercially available poly(vinylidene difluoride) (PVDF) and chemically modifying it from its native hydrophobicity for compatibility with the hydrophilic trichlorfon (TCF) analyte, a dangerous pesticide requiring food monitoring. PVDF's long chains knot similar to crosslinking networks. The constructed device exhibits linear detection from 0 to 250 ppb and an LOD equal to 4.63 ppb. An imprinting factor, ratio of MIP selectivity to NIP selectivity, of 3.2 was reported after optimizing the PVDF to TCF amounts. Selectivity was further demonstrated through sensor performance with TCF versus chemically similar pesticides. Biosensor performance was evaluated in water and iceberg lettuce samples. Evaluation of the adsorption isotherms revealed the MIP layer was comprised of homogenous and heterogenous binding sites, after data fitting best matched the Redlich-Peterson model. The researchers conclude their facile synthesis lowers costs.

Another relevant contribution to gravimetric biosensor transduction was made by Tang et al. The researchers report novel construction of a Love-type SAW biosensor on which an MIP recognizes prostate-specific membrane antigen (PSMA)

(206). This MIP was fabricated via reversible addition/fragmentation chain transfer (RAFT) precipitation polymerization so that resulting polymer brushes enhanced hydrophilicity. Acrylamide and 2(dimethylamino) ethyl methacrylate were the functional monomers. The synergistic combination of Love sensor with modified MIP results in sensitive aqueous analyte detection. The device exhibits an LOD equal to 0.013 ng mL^{-1} and good linear performance from 0.01 to 100 ng mL^{-1}. The device was selective when assessed against three other analytes. Calibration of PSMA detection was performed in spiked PBS. Trials in mouse serum were conducted to demonstrate applicability to real samples.

One final gravimetric case study describes incorporation of MIPs for NEMS devices. Researchers use MIPs to assess their resistance to damage under formidable wet-etching conditions, like soft lithography, microspotting, photolithography, and two-photon stereolithography, which is characteristic of MEMS fabrication (207). Such processes are detrimental in conventional binding strategies. NEMS devices access ultra-sensitive performance via excellent mass resolution, label-free detection, and highly-integrated operation. The investigators address NEMS obstacles like inefficient transduction integration, low response time associated with miniaturization, and poor multiplexed functionalization. MIP coated cantilevers are selective for the target analyte, the fluorescent amino acid dansyl-L-phenylalanine (DLP), compared to NIP coated cantilevers. The detection performance of eight cantilevers was narrowly uniform. A sensitivity range was not reported due to the low molecular weight of the target and poorly controlled cantilever functionalization. The analyte spiked samples were dispersed in acetonitrile.

Conclusion and Future Directions

Sophisticated MIP efforts abandon top-down fabrication, like milling down bulk polymers, for bottom-up nanoscale formulations. Thin MIP layers and nanomaterials improve mass transfer addressing challenges related to effective template removal and analyte binding (46). Conductive nanomaterials and MIPs synergistically improve biosensor efficacy by reducing the latter's insulating nature and mitigating the former's inherent dispersal and toxicity challenges (167). Another MIP biosensor challenge, limited selection of monomers and crosslinkers for custom analyte binding, is mitigated through intelligent application of computer modeling (103) and adoption of SNMs as nanocarrier (166). These vanishing MIP challenges are further offset by their advantages when compared to conventional binding (Table 1): sensitivity, stability, expense, and others (96).

Based on these outcomes, recommendations are offered toward advancing the field. First, diligence is needed in NIP fabrication for appropriate MIP comparison. NIPs should be produced with an analog template rather than no template, just as the MIP is produced with a template (104). Next, ECM devices (Fig. 1d) are successful and, therefore, safe to dedicate more research to. However, recent advances in MIPs composited with nanomaterials opens the door to revisit routinely overlooked strategies, like gravimetric transduction. It is noteworthy that MIP-based magnetic transduction nanobiosensors are absent at the time of writing (43), despite successes with conventional binding (29). Magnetics researchers have much to offer this field besides sample purification. GMR, SQUID, Hall Effect, and other magnetic transduction strategies, coupled with MIP selectivity, may pave the way to widespread POCT.

Acknowledgement

This work is supported by a Veterans Affairs Merit Review grant (BX002668) to Dr. Subhra Mohapatra, and Research Career Scientist Awards to Dr. Subhra Mohapatra (IK6BX004212) and Dr. Shyam Mohapatra (IK6 BX003778). Though this report is based upon work supported, in part, by the Department of Veterans Affairs, Veterans Health Administration, Office of Research and Development, the contents of this report do not represent the views of the Department of Veterans Affairs or the United States Government. Additionally, a special thank you is extended to Ms. Christen Bouchard for her valuable proof-reading services.

Conflict of Interests

The authors declare that they have no competing interest.

References

1. Wang HD, Abajobir AA, Abate KH, Abbafati C, Abbas KM, Abd-Allah F, Abera SF, Abraha HN, Abu-Raddad LJ, Abu-Rmeileh NME. Global, regional, and national under-5 mortality, adult mortality, age-specific mortality, and life expectancy, 1970-2016: a systematic analysis for the Global Burden of Disease Study 2016. Lancet 2017; 390:1084-1150
2. Barber RM, Fullman N, Sorensen RJ, Bollyky T, McKee M, Nolte E, Abajobir AA, Abate KH, Abbafati C, Abbas KM. Healthcare Access and Quality Index based on mortality from causes amenable to personal health care in 195 countries and territories, 1990–2015: a novel analysis from the Global Burden of Disease Study 2015. The Lancet 2017; 390:231-266
3. Zhao J, Yuan Q, Wang H, Liu W, Liao X, Su Y, Wang X, Yuan J, Li T, Li J, Qian S, Hong C, Wang F, Liu Y, Wang Z, He Q, Li Z, He B, Zhang T, Fu Y, Ge S, Liu L, Zhang J, Xia N, Zhang Z. Antibody responses to SARS-CoV-2 in patients of novel coronavirus disease 2019. Clin Infect Dis 2020.
4. Yu X, Sun S, Shi Y, Wang H, Zhao R, Sheng J. SARS-CoV-2 viral load in sputum correlates with risk of COVID-19 progression. Crit Care 2020; 24:170
5. Palant CE, Chawla LS, Faselis C, Li P, Pallone TL, Kimmel PL, Amdur RL. High serum creatinine nonlinearity: a renal vital sign? Am J Physiol Renal Physiol 2016; 311:F305-9
6. Canovas R, Cuartero M, Crespo GA. Modern creatinine (Bio)sensing: Challenges of point-of-care platforms. Biosens Bioelectron 2019; 130:110-124
7. Qin X, Rui J, Xia Y, Mu H, Song SH, Raja Aziddin RE, Miles G, Sun Y, Chun S. Multi-center Performance Evalu-

ations of Tacrolimus and Cyclosporine Electrochemiluminescence Immunoassays in the Asia-Pacific Region. Ann Lab Med 2018; 38:85-94
8. Romano P, da Luz Fernandes M, de Almeida Rezende Ebner P, Duarte de Oliveira N, Mitsue Okuda L, Agena F, Mendes ME, Massakazu Sumita N, Coelho V, David-Neto E, Zocoler Galante N. UPLC-MS/MS assay validation for tacrolimus quantitative determination in peripheral blood T CD4+ and B CD19+ lymphocytes. J Pharm Biomed Anal 2018; 152:306-314
9. Obama B. United States Health Care Reform: Progress to Date and Next Steps. JAMA 2016; 316:525-32
10. Papanicolas I, Woskie LR, Jha AK. Health Care Spending in the United States and Other High-Income Countries. JAMA 2018; 319:1024-1039
11. Bhattarai J, Bentley J, Morean W, Wegener ST, Pollack Porter KM. Promoting equity at the population level: Putting the foundational principles into practice through disability advocacy. Rehabil Psychol 2020; 65:87-100
12. Bethell CD, Kogan MD, Strickland BB, Schor EL, Robertson J, Newacheck PW. A national and state profile of leading health problems and health care quality for US children: key insurance disparities and across-state variations. Acad Pediatr 2011; 11:S22-33
13. Brown CE, Engelberg RA, Sharma R, Downey L, Fausto JA, Sibley J, Lober W, Khandelwal N, Loggers ET, Curtis JR. Race/Ethnicity, Socioeconomic Status, and Healthcare Intensity at the End of Life. J Palliat Med 2018; 21:1308-1316
14. Hafeez H, Zeshan M, Tahir MA, Jahan N, Naveed S. Health Care Disparities Among Lesbian, Gay, Bisexual, and Transgender Youth: A Literature Review. Cureus 2017; 9:e1184
15. Quesada-Gonzalez D and Merkoci A. Nanomaterial-based devices for point-of-care diagnostic applications. Chem Soc Rev 2018; 47:4697-4709
16. Mahato K, Maurya PK, Chandra P. Fundamentals and commercial aspects of nanobiosensors in point-of-care clinical diagnostics. 3 Biotech 2018; 8:149
17. Nayak S, Blumenfeld NR, Laksanasopin T, Sia SK. Point-of-Care Diagnostics: Recent Developments in a Connected Age. Anal Chem 2017; 89:102-123
18. Chan HN, Tan MJA, Wu H. Point-of-care testing: applications of 3D printing. Lab Chip 2017; 17:2713-2739
19. Lee HN, Ryu JS, Shin C, Chung HJ. A Carbon-Dot-Based Fluorescent Nanosensor for Simple Visualization of Bacterial Nucleic Acids. Macromol Biosci 2017; 17:
20. Sun AC, Yao C, Venkatesh AG, Hall DA. An Efficient Power Harvesting Mobile Phone-Based Electrochemical Biosensor for Point-of-Care Health Monitoring. Sens Actuators B Chem 2016; 235:126-135
21. Bhalla N, Jolly P, Formisano N, Estrela P. Introduction to biosensors. Essays Biochem 2016; 60:1-8
22. Bellan LM, Wu D, Langer RS. Current trends in nanobiosensor technology. Wiley Interdiscip Rev Nanomed Nanobiotechnol 2011; 3:229-46
23. Sagadevan S and Periasamy M. Recent Trends in Nanobiosensors and Their Applications - a Review. Rev Adv Mater Sci 2014; 36:62-69
24. Higgins IJ, Swain A, Turner APF. Principles and application of biosensors in microbiology. J Appl Bacteriol 1987; 63:93S-104S
25. Cho IH, Lee J, Kim J, Kang MS, Paik JK, Ku S, Cho HM, Irudayaraj J, Kim DH. Current Technologies of Electrochemical Immunosensors: Perspective on Signal Amplification. Sensors (Basel) 2018; 18:
26. Grieshaber D, MacKenzie R, Voros J, Reimhult E. Electrochemical Biosensors - Sensor Principles and Architectures. Sensors-Basel 2008; 8:1400-1458
27. Chen C and Wang J. Optical biosensors: an exhaustive and comprehensive review. Analyst 2020; 145:1605-1628
28. Ramsden JJ. Optical Biosensors. J Mol Recognit 1997; 10:109-120
29. Denmark DJ, Bustos-Perez X, Swain A, Phan M-H, Mohapatra S, Mohapatra SS. Readiness of Magnetic Nanobiosensors for Point-of-Care Commercialization. J Electron Mater 2019; 48:4749-4761
30. Giouroudi I and Kokkinis G. Recent Advances in Magnetic Microfluidic Biosensors. Nanomaterials (Basel) 2017; 7:
31. Yakovleva M, Bhand S, Danielsson B. The enzyme thermistor--a realistic biosensor concept. A critical review. Anal Chim Acta 2013; 766:1-12
32. Xie B, Ramanathan K, Danielsson B. Mini / micro thermal biosensors and other related devices for biochemical / clinical analysis and monitoring. Trac-Trend Anal Chem 2000; 19:340-349
33. Arlett JL, Myers EB, Roukes ML. Comparative advantages of mechanical biosensors. Nat Nanotechnol 2011; 6:203-15
34. Willner I, Patolsky F, Weizmann Y, Willner B. Amplified detection of single-base mismatches in DNA using micro gravimetric quartz-crystal-microbalance transduction. Talanta 2002; 56:847-856
35. Conroy PJ, Hearty S, Leonard P, O'Kennedy RJ. Antibody production, design and use for biosensor-based applications. Semin Cell Dev Biol 2009; 20:10-26
36. Morales MA and Halpern JM. Guide to Selecting a Biorecognition Element for Biosensors. Bioconjug Chem 2018; 29:3231-3239
37. Dou L, Zhao B, Bu T, Zhang W, Huang Q, Yan L, Huang L, Wang Y, Wang J, Zhang D. Highly sensitive detection of a small molecule by a paired labels recognition system based lateral flow assay. Anal Bioanal Chem 2018; 410:3161-3170
38. Morgan CL, Newman DJ, Price CP. Immunosensors: Technology and Opportunities in Laboratory Medicine. Clin Chem 1996; 42:193-209
39. Smolinska-Kempisty K, Guerreiro A, Canfarotta F, Caceres C, Whitcombe MJ, Piletsky S. A comparison of the performance of molecularly imprinted polymer nanoparticles for small molecule targets and antibodies in the ELISA format. Sci Rep 2016; 6:37638
40. Hopkins NAE, in Antibody Engineering for Biosensor Applications, ed. By Z. M. (Springer, New York, NY, 2010),
41. Erturk G and Mattiasson B. Molecular Imprinting Techniques Used for the Preparation of Biosensors. Sensors (Basel) 2017; 17:
42. Whitcombe MJ, Kirsch N, Nicholls IA. Molecular imprinting science and technology: a survey of the literature for the years 2004-2011. J Mol Recognit 2014; 27:297-401

43. Li R, Feng Y, Pan G, Liu L. Advances in Molecularly Imprinting Technology for Bioanalytical Applications. Sensors (Basel) 2019; 19:
44. Selvolini G and Marrazza G. MIP-Based Sensors: Promising New Tools for Cancer Biomarker Determination. Sensors (Basel) 2017; 17:
45. Safaryan AHM, Smith AM, Bedwell TS, Piletska EV, Canfarotta F, Piletsky SA. Optimisation of the preservation conditions for molecularly imprinted polymer nanoparticles specific for trypsin. Nanoscale Advances 2019; 1:3709-3714
46. Chen L, Wang X, Lu W, Wu X, Li J. Molecular imprinting: perspectives and applications. Chem Soc Rev 2016; 45:2137-211
47. BelBruno JJ. Molecularly Imprinted Polymers. Chem Rev 2019; 119:94-119
48. Ge Y, Butler B, Mirza F, Habib-Ullah S, Fei D. Smart molecularly imprinted polymers: recent developments and applications. Macromol Rapid Commun 2013; 34:903-15
49. Wang C, Howell M, Raulji P, Davis Y, Mohapatra S. Preparation and Characterization of Molecularly Imprinted Polymeric Nanoparticles for Atrial Natriuretic Peptide (ANP). Adv Funct Mater 2011; 21:4423-4429
50. Huang H, Wang X, Ge H, Xu M. Multifunctional Magnetic Cellulose Surface-Imprinted Microspheres for Highly Selective Adsorption of Artesunate. ACS Sustainable Chemistry & Engineering 2016; 4:3334-3343
51. Wang HY, Cao PP, He ZY, He XW, Li WY, Li YH, Zhang YK. Targeted imaging and targeted therapy of breast cancer cells via fluorescent double template-imprinted polymer coated silicon nanoparticles by an epitope approach. Nanoscale 2019; 11:17018-17030
52. Kubo T, Tachibana K, Naito T, Mukai S, Akiyoshi K, Balachandran J, Otsuka K. Magnetic Field Stimuli-Sensitive Drug Release Using a Magnetic Thermal Seed Coated with Thermal-Responsive Molecularly Imprinted Polymer. ACS Biomaterials Science & Engineering 2018; 5:759-767
53. Griffete N, Fresnais J, Espinosa A, Wilhelm C, Bee A, Menager C. Design of magnetic molecularly imprinted polymer nanoparticles for controlled release of doxorubicin under an alternative magnetic field in athermal conditions. Nanoscale 2015; 7:18891-6
54. Liu LT, Chen MJ, Yang HL, Huang ZJ, Tang Q, Chow CF, Gong CB, Zu MH, Xiao B. An NIR-light-responsive surface molecularly imprinted polymer for photoregulated drug release in aqueous solution through porcine tissue. Mater Sci Eng C Mater Biol Appl 2020; 106:110253
55. Cruz JC, de Faria HD, Figueiredo EC, Queiroz MEC. Restricted access carbon nanotube for microextraction by packed sorbent to determine antipsychotics in plasma samples by high-performance liquid chromatography-tandem mass spectrometry. Anal Bioanal Chem 2020; 412:2465-2475
56. Chen L, Zhang X, Xu Y, Du X, Sun X, Sun L, Wang H, Zhao Q, Yu A, Zhang H, Ding L. Determination of fluoroquinolone antibiotics in environmental water samples based on magnetic molecularly imprinted polymer extraction followed by liquid chromatography-tandem mass spectrometry. Anal Chim Acta 2010; 662:31-8
57. Xie H, Ji W, Liu D, Liu W, Wang D, Lv R, Wang X. Surface molecularly imprinted polymers with dummy templates for the separation of dencichine from Panax notoginseng. RSC Advances 2015; 5:48885-48892
58. Zhao WR, Xu YH, Kang TF, Zhang X, Liu H, Ming AJ, Cheng SY, Wei F. Sandwich magnetically imprinted immunosensor for electrochemiluminescence ultrasensing diethylstilbestrol based on enhanced luminescence of Ru@SiO2 by CdTe@ZnS quantum dots. Biosens Bioelectron 2020; 155:112102
59. Lu YC, Guo MH, Mao JH, Xiong XH, Liu YJ, Li Y. Preparation of core-shell magnetic molecularly imprinted polymer nanoparticle for the rapid and selective enrichment of trace diuron from complicated matrices. Ecotoxicol Environ Saf 2019; 177:66-76
60. Ndunda EN and Mizaikoff B. Molecularly imprinted polymers for the analysis and removal of polychlorinated aromatic compounds in the environment: a review. Analyst 2016; 141:3141-56
61. Bumbudsanpharoke N and Ko S. Nanomaterial-based optical indicators: Promise, opportunities, and challenges in the development of colorimetric systems for intelligent packaging. Nano Research 2019; 12:489-500
62. Gutiérrez TJ, Ponce AG, Alvarez VA. Nano-clays from natural and modified montmorillonite with and without added blueberry extract for active and intelligent food nanopackaging materials. Mater Chem Phys 2017; 194:283-292
63. Jayakumar A, K VH, T SS, Joseph M, Mathew S, G P, Nair IC, E KR. Starch-PVA composite films with zinc-oxide nanoparticles and phytochemicals as intelligent pH sensing wraps for food packaging application. Int J Biol Macromol 2019; 136:395-403
64. Nguyen-Tri P, Tran HN, Plamondon CO, Tuduri L, Vo D-VN, Nanda S, Mishra A, Chao H-P, Bajpai AK. Recent progress in the preparation, properties and applications of superhydrophobic nano-based coatings and surfaces: A review. Progress in Organic Coatings 2019; 132:235-256
65. Yamauchi G, Riko Y, Yasuno Y, Shimizu T, Funakoshi N. Water-repellent coating for mobile phone microphones. Surface Coatings International Part B-Coatings Transactions 2005; 88:281-283
66. Sun J, Shi X, Du Y, Wu Y. A robust, flexible superhydrophobic sheet fabricated by in situ growth of micro-nano-SiO2 particles from cured silicone rubber. Journal of Sol-Gel Science and Technology 2019; 91:208-215
67. Peters RJB, Bouwmeester H, Gottardo S, Amenta V, Arena M, Brandhoff P, Marvin HJP, Mech A, Moniz FB, Pesudo LQ, Rauscher H, Schoonjans R, Undas AK, Vettori MV, Weigel S, Aschberger K. Nanomaterials for products and application in agriculture, feed and food. Trends Food Sci Technol 2016; 54:155-164
68. Riedle S, Wills JW, Miniter M, Otter DE, Singh H, Brown AP, Micklethwaite S, Rees P, Jugdaohsingh R, Roy NC, Hewitt RE, Powell JJ. A Murine Oral-Exposure Model for Nano- and Micro-Particulates: Demonstrating Human Relevance with Food-Grade Titanium Dioxide. Small 2020; 16:e2000486
69. Ojagh SM and Hasani S. Characteristics and oxidative

stability of fish oil nano-liposomes and its application in functional bread. Journal of Food Measurement and Characterization 2018; 12:1084-1092
70. Ahmadi MH, Ghazvini M, Alhuyi Nazari M, Ahmadi MA, Pourfayaz F, Lorenzini G, Ming T. Renewable energy harvesting with the application of nanotechnology: A review. International Journal of Energy Research 2018; 43:1387-1410
71. Kawawaki T, Negishi Y, Kawasaki H. Photo/electrocatalysis and photosensitization using metal nanoclusters for green energy and medical applications. Nanoscale Advances 2020; 2:17-36
72. Thaver Y, Oseni SO, Kaviyarasu K, Dwivedi RP, Mola GT. Metal nano-composite assisted photons harvesting in thin film organic photovoltaic. Physica B: Condensed Matter 2020; 582:411844
73. Aziz ZAA, Mohd-Nasir H, Ahmad A, Mohd Setapar SH, Peng WL, Chuo SC, Khatoon A, Umar K, Yaqoob AA, Mohamad Ibrahim MN. Role of Nanotechnology for Design and Development of Cosmeceutical: Application in Makeup and Skin Care. Front Chem 2019; 7:739
74. Mohd Taib SH, Abd Gani SS, Ab Rahman MZ, Basri M, Ismail A, Shamsudin R. Formulation and process optimizations of nano-cosmeceuticals containing purified swiftlet nest. RSC Advances 2015; 5:42322-42328
75. Kalouta K, Eleni P, Boukouvalas C, Vassilatou K, Krokida M. Dynamic mechanical analysis of novel cosmeceutical facial creams containing nano-encapsulated natural plant and fruit extracts. J Cosmet Dermatol 2020; 19:1146-1154
76. Denmark DJ, Bradley J, Mukherjee D, Alonso J, Shakespeare S, Bernal N, Phan MH, Srikanth H, Witanachchi S, Mukherjee P. Remote triggering of thermoresponsive PNIPAM by iron oxide nanoparticles. Rsc Adv 2016; 6:5641-5652
77. Denmark DJ, Hyde RH, Gladney C, Phan MH, Bisht KS, Srikanth H, Mukherjee P, Witanachchi S. Photopolymerization-based synthesis of iron oxide nanoparticle embedded PNIPAM nanogels for biomedical applications. Drug Deliv 2017; 24:1317-1324
78. Lim B-K, Tighe EC, Kong SD. The use of magnetic targeting for drug delivery into cardiac myocytes. Journal of Magnetism and Magnetic Materials 2019; 473:21-25
79. Jazayeri MH, Amani H, Pourfatollah AA, Pazoki-Toroudi H, Sedighimoghaddam B. Various methods of gold nanoparticles (GNPs) conjugation to antibodies. Sensing and Bio-Sensing Research 2016; 9:17-22
80. Elahi N, Kamali M, Baghersad MH. Recent biomedical applications of gold nanoparticles: A review. Talanta 2018; 184:537-556
81. Saleh M, Soliman H, Haenen O, El-Matbouli M. Antibody-coated gold nanoparticles immunoassay for direct detection of Aeromonas salmonicida in fish tissues. J Fish Dis 2011; 34:845-52
82. Kim KB, Kim YW, Lim SK, Roh TH, Bang DY, Choi SM, Lim DS, Kim YJ, Baek SH, Kim MK, Seo HS, Kim MH, Kim HS, Lee JY, Kacew S, Lee BM. Risk assessment of zinc oxide, a cosmetic ingredient used as a UV filter of sunscreens. J Toxicol Environ Health B Crit Rev 2017; 20:155-182
83. Sanches PL, Souza W, Gemini-Piperni S, Rossi AL, Scapin S, Midlej V, Sade Y, Leme AFP, Benchimol M, Rocha LA, Carias RBV, Borojevic R, Granjeiro JM, Ribeiro AR. Rutile nano–bio-interactions mediate dissimilar intracellular destiny in human skin cells. Nanoscale Advances 2019; 1:2216-2228
84. Irshad M, Iqbal N, Mujahid A, Afzal A, Hussain T, Sharif A, Ahmad E, Athar MM. Molecularly Imprinted Nanomaterials for Sensor Applications. Nanomaterials (Basel) 2013; 3:615-637
85. Komiyama M, Mori T, Ariga K. Molecular Imprinting: Materials Nanoarchitectonics with Molecular Information. Bull Chem Soc Jpn 2018; 91:1075-1111
86. Jain KK, The Handbook Of Nanomedicine - 3rd ed., 3 (Humana Press, 2017), pp.
87. Burgess R, Understanding Nanomedicine - An Introductory Textbook, (Pan Stanford Publishing Pte. Ltd., Singapore, 2012), pp.
88. Roy H, Nayak BS, Rahaman SA, Characterization and Biology of Nanomaterials for Drug Delivery - Nanoscience and Nanotechnology in Drug Delivery, (Elsevier, Amsterdam, 2019), pp. 447-456.
89. Holzinger M, Le Goff A, Cosnier S. Nanomaterials for biosensing applications: a review. Front Chem 2014; 2:63
90. Moreno-Bondi M, Navarro-Villoslada F, Benito-Pena E, Urraca J. Molecularly Imprinted Polymers as Selective Recognition Elements in Optical Sensing. Curr Anal Chem 2008; 4:316-340
91. Niu M, Pham-Huy C, He H. Core-shell nanoparticles coated with molecularly imprinted polymers: a review. Microchim Acta 2016; 183:2677-2695
92. Poma A, Turner AP, Piletsky SA. Advances in the manufacture of MIP nanoparticles. Trends Biotechnol 2010; 28:629-37
93. Yoshimatsu K, Reimhult K, Krozer A, Mosbach K, Sode K, Ye L. Uniform molecularly imprinted microspheres and nanoparticles prepared by precipitation polymerization: the control of particle size suitable for different analytical applications. Anal Chim Acta 2007; 584:112-21
94. Beyazit S, Tse Sum Bui B, Haupt K, Gonzato C. Molecularly imprinted polymer nanomaterials and nanocomposites by controlled/living radical polymerization. Progress in Polymer Science 2016; 62:1-21
95. Li X, Liu H, Deng Z, Chen W, Li T, Zhang Y, Zhang Z, He Y, Tan Z, Zhong S. PEGylated Thermo-Sensitive Bionic Magnetic Core-Shell Structure Molecularly Imprinted Polymers Based on Halloysite Nanotubes for Specific Adsorption and Separation of Bovine Serum Albumin. Polymers (Basel) 2020; 12:
96. Chen L, Xu S, Li J. Recent advances in molecular imprinting technology: current status, challenges and highlighted applications. Chem Soc Rev 2011; 40:2922-42
97. Fang GZ, Feng JJ, Yan YF, Liu CC, Wang S. Highly Selective Determination of Chrysoidine in Foods Through a Surface Molecularly Imprinted Sol-Gel Polymer Solid-Phase Extraction Coupled with HPLC. Food Analytical Methods 2014; 7:345-351
98. Chen W, Ma Y, Pan JM, Meng ZH, Pan GQ, Sellergren B. Molecularly Imprinted Polymers with Stimuli-Respon-

sive Affinity: Progress and Perspectives. Polymers 2015; 7:1689-1715
99. Dinc M, Esen C, Mizaikoff B. Recent advances on core–shell magnetic molecularly imprinted polymers for bio-macromolecules. TrAC Trends in Analytical Chemistry 2019; 114:202-217
100. Miyata T, Jige M, Nakaminami T, Uragami T. Tumor marker-responsive behavior of gels prepared by biomolecular imprinting. Proc Natl Acad Sci U S A 2006; 103:1190-1193
101. Watanabe M, Akahoshi T, Tabata Y, Nakayama D. Molecular Specific Swelling Change of Hydrogels in Accordance with the Concentration of Guest Molecules. J Am Chem Soc 1998; 120:5577-5578
102. Hien Nguyen T and Ansell RJ. N-isopropylacrylamide as a functional monomer for noncovalent molecular imprinting. J Mol Recognit 2012; 25:1-10
103. Smolinska-Kempisty K, Ahmad OS, Guerreiro A, Karim K, Piletska E, Piletsky S. New potentiometric sensor based on molecularly imprinted nanoparticles for cocaine detection. Biosens Bioelectron 2017; 96:49-54
104. Ndunda EN. Molecularly imprinted polymers-A closer look at the control polymer used in determining the imprinting effect: A mini review. J Mol Recognit 2020.e2855
105. Lu Z, Li Y, Liu T, Wang G, Sun M, Jiang Y, He H, Wang Y, Zou P, Wang X, Zhao Q, Rao H. A dual-template imprinted polymer electrochemical sensor based on AuNPs and nitrogen-doped graphene oxide quantum dots coated on NiS2/biomass carbon for simultaneous determination of dopamine and chlorpromazine. Chem Eng J 2020; 389:124417
106. Wu Y, Deng P, Tian Y, Ding Z, Li G, Liu J, Zuberi Z, He Q. Rapid recognition and determination of tryptophan by carbon nanotubes and molecularly imprinted polymer-modified glassy carbon electrode. Bioelectrochemistry 2020; 131:107393
107. Rebelo T, Costa R, Brandao A, Silva AF, Sales MGF, Pereira CM. Molecularly imprinted polymer SPE sensor for analysis of CA-125 on serum. Anal Chim Acta 2019; 1082:126-135
108. Wang Y, Li H, Wang X, Wang Z, Wang M, Li Y, Wang Q. Preparation of a high-performance magnetic molecularly imprinted sensor for SERS detection of cyfluthrin in river. J Raman Spectrosc 2019.
109. Hussain M, Kotova K, Lieberzeit PA. Molecularly Imprinted Polymer Nanoparticles for Formaldehyde Sensing with QCM. Sensors (Basel) 2016; 16:
110. Cennamo N, Zeni L, Pesavento M, Marchetti S, Marletta V, Baglio S, Graziani S, Pistorio A, Ando B. A Novel Sensing Methodology to Detect Furfural in Water, Exploiting MIPs, and Inkjet-Printed Optical Waveguides. IEEE Transactions on Instrumentation and Measurement 2019; 68:1582-1589
111. Zhao P, Liu H, Zhang L, Zhu P, Ge S, Yu J. Paper-Based SERS Sensing Platform Based on 3D Silver Dendrites and Molecularly Imprinted Identifier Sandwich Hybrid for Neonicotinoid Quantification. ACS Appl Mater Interfaces 2020; 12:8845-8854
112. Chen S, Gan N, Zhang H, Hu F, Li T, Cui H, Cao Y, Jiang Q. A Portable and Antibody-free Sandwich Assay for Determination of Chloramphenicol in Food Based on a Personal Glucose Meter. Anal Bioanal Chem 2015; 407:2499-2507
113. National Nanotechnology Initiative Glossary. https://www.nano.gov/about-nni/glossary. Accessed June 5, 2020.
114. Sefcovicova J and Tkac J. Application of nanomaterials in microbial-cell biosensor constructions. Chem Pap 2015; 69:42-53
115. Nichols G, Byard S, Bloxham MJ, Botterill J, Dawson NJ, Dennis A, Diart V, North NC, Sherwood JD. A Review of the Terms Agglomerate and Aggregate with a Recommendation for Nomenclature Used in Powder and Particle Characterization. J Pharm Sci 2002; 91:2103-2109
116. Dazon C, Witschger O, Bau S, Fierro V, Llewellyn PL. Toward an operational methodology to identify industrial-scaled nanomaterial powders with the volume specific surface area criterion. Nanoscale Advances 2019; 1:3232-3242
117. Tran QH, Nguyen VQ, Le A-T. Corrigendum: Silver nanoparticles: synthesis, properties, toxicology, applications and perspectives (Adv. Nat. Sci: Nanosci. Nanotechnol 4033001). Advances in Natural Sciences: Nanoscience and Nanotechnology 2018; 9:049501
118. Wang X, Sun W, Yang W, Gao S, Sun C, Li Q. Mesoporous silica-protected silver nanoparticle disinfectant with controlled Ag+ ion release, efficient magnetic separation, and effective antibacterial activity. Nanoscale Advances 2019; 1:840-848
119. Iravani S, Korbekandi H, Mirmohammadi S, B Z. Synthesis of silver nanoparticles: chemical, physical, and biological methods. Res Pharm Sci 2014; 9:385-406
120. Coll C, Notter D, Gottschalk F, Sun T, Som C, Nowack B. Probabilistic environmental risk assessment of five nanomaterials (nano-TiO2, nano-Ag, nano-ZnO, CNT, and fullerenes). Nanotoxicology 2016; 10:436-44
121. Recordati C, De Maglie M, Bianchessi S, Argentiere S, Cella C, Mattiello S, Cubadda F, Aureli F, D'Amato M, Raggi A, Lenardi C, Milani P, Scanziani E. Tissue distribution and acute toxicity of silver after single intravenous administration in mice: nano-specific and size-dependent effects. Part Fibre Toxicol 2016; 13:12
122. Yao Z, Yang X, Liu X, Yang Y, Hu Y, Zhao Z. Electrochemical quercetin sensor based on a nanocomposite consisting of magnetized reduced graphene oxide, silver nanoparticles and a molecularly imprinted polymer on a screen-printed electrode. Mikrochim Acta 2017; 185:70
123. Hu M, Chen J, Li ZY, Au L, Hartland GV, Li X, Marquez M, Xia Y. Gold nanostructures: engineering their plasmonic properties for biomedical applications. Chem Soc Rev 2006; 35:1084-94
124. Romo-Herrera JM, Alvarez-Puebla RA, Liz-Marzan LM. Controlled assembly of plasmonic colloidal nanoparticle clusters. Nanoscale 2011; 3:1304-15
125. Kumar KK, Devendiran M, Kalaivani RA, Narayanan SS. Enhanced electrochemical sensing of dopamine in the presence of AA and UA using a curcumin functionalized gold nanoparticle modified electrode. New Journal of Chemistry 2019; 43:19003-19013
126. Shriver-Lake LC, Donner B, Edelstein R, Breslin K, Bhatia SK, Ligler FS. Antibody Immobilization using Het-

erobifunctional Crosslinkers. Biosens Bioelectron 1997; 12:1101-1106
127. Ma LY, Miao SS, Lu FF, Wu MS, Lu YC, Yang H. Selective Electrochemical Determination of Salicylic Acid in Wheat Using Molecular Imprinted Polymers. Anal Lett 2017; 50:2369-2385
128. Wang J, Li J, Zeng C, Qu Q, Wang M, Qi W, Su R, He Z. Sandwich-Like Sensor for the Highly Specific and Reproducible Detection of Rhodamine 6G on a Surface-Enhanced Raman Scattering Platform. ACS Appl Mater Interfaces 2020; 12:4699-4706
129. Xing R, Wen Y, Dong Y, Wang Y, Zhang Q, Liu Z. Dual Molecularly Imprinted Polymer-Based Plasmonic Immunosandwich Assay for the Specific and Sensitive Detection of Protein Biomarkers. Anal Chem 2019; 91:9993-10000
130. Lv Y, Tan T, Svec F. Molecular imprinting of proteins in polymers attached to the surface of nanomaterials for selective recognition of biomacromolecules. Biotechnol Adv 2013; 31:1172-86
131. Maiti D, Tong X, Mou X, Yang K. Carbon-Based Nanomaterials for Biomedical Applications: A Recent Study. Front Pharmacol 2018; 9:1401
132. Alwarappan S, Cissell K, Dixit S, Mohapatra S, Li CZ. Chitosan-Modified Graphene Electrodes for DNA Mutation Analysis. J Electroanal Chem (Lausanne) 2012; 686:69-72
133. Alwarappan S, Singh SR, Pillai S, Kumar A, Mohapatra S. Direct Electrochemistry of Glucose Oxidase at a Gold Electrode Modified with Graphene Nanosheets. Anal Lett 2012; 45:746-753
134. Ertugrul Uygun HD, Uygun ZO, Canbay E, Gi Rgi NSF, Sezer E. Non-invasive cortisol detection in saliva by using molecularly cortisol imprinted fullerene-acrylamide modified screen printed electrodes. Talanta 2020; 206:120225
135. Han S, Su L, Zhai M, Ma L, Liu S, Teng Y. A molecularly imprinted composite based on graphene oxide for targeted drug delivery to tumor cells. Journal of Materials Science 2018; 54:3331-3341
136. Han S, Teng F, Wang Y, Su L, Leng Q, Jiang H. Drug-loaded dual targeting graphene oxide-based molecularly imprinted composite and recognition of carcino-embryonic antigen. RSC Advances 2020; 10:10980-10988
137. Prasad BB, Singh R, Kumar A. Synthesis of fullerene (C60-monoadduct)-based water-compatible imprinted micelles for electrochemical determination of chlorambucil. Biosens Bioelectron 2017; 94:115-123
138. Lu AH, Salabas EL, Schuth F. Magnetic nanoparticles: synthesis, protection, functionalization, and application. Angew Chem Int Ed Engl 2007; 46:1222-44
139. Phan MH, Alonso J, Khurshid H, Lampen-Kelley P, Chandra S, Stojak Repa K, Nemati Z, Das R, Iglesias O, Srikanth H. Exchange Bias Effects in Iron Oxide-Based Nanoparticle Systems. Nanomaterials (Basel) 2016; 6:
140. Denmark DJ, Photopolymerization Synthesis of Magnetic Nanoparticle Embedded Nanogels for Targeted Biotherapeutic Delivery, in Department of Physics. 2017, University of South Florida: USF Scholar Commons. p. 214
141. Alonso J, Barandiarán JM, Fernández Barquín L, García-Arribas A, in Magnetic Nanoparticles, Synthesis, Properties, and Applications, ed. By A.A. El-Gendy, J.M. Barandiarán, and R.L. Hadimani (Elsevier, 2018), 1-40.
142. Wu K, Su D, Liu J, Saha R, Wang JP. Magnetic nanoparticles in nanomedicine: a review of recent advances. Nanotechnology 2019; 30:502003
143. Denmark DJ, Mukherjee D, Bradley J, Witanachchi S, Mukherjee P. Systematic Study on the Remote Triggering of Thermo-Responsive Hydrogels Using RF Heating of Fe3O4 Nanoparticles. MRS Proceedings 2015; 1718:35-40
144. Smith JE, Sapsford KE, Tan W, Ligler FS. Optimization of antibody-conjugated magnetic nanoparticles for target preconcentration and immunoassays. Anal Biochem 2011; 410:124-32
145. Chen YT, Kolhatkar AG, Zenasni O, Xu S, Lee TR. Biosensing Using Magnetic Particle Detection Techniques. Sensors (Basel) 2017; 17:
146. Lin G, Makarov D, Schmidt OG. Magnetic sensing platform technologies for biomedical applications. Lab Chip 2017; 17:1884-1912
147. Llandro J, Palfreyman JJ, Ionescu A, Barnes CH. Magnetic biosensor technologies for medical applications: a review. Med Biol Eng Comput 2010; 48:977-98
148. Ludwig F, Heim E, Mauselein S, Eberbeck D, Schilling M. Magnetorelaxometry of magnetic nanoparticles with fluxgate magnetometers for the analysis of biological targets. J Magn Magn Mater 2005; 293:690-695
149. Nabaei V, Chandrawati R, Heidari H. Magnetic biosensors: Modelling and simulation. Biosens Bioelectron 2018; 103:69-86
150. Phan MH and Peng HX. Giant magnetoimpedance materials: Fundamentals and applications. Prog Mater Sci 2008; 53:323-420
151. Rocha-Santos TAP. Sensors and biosensors based on magnetic nanoparticles. Trac-Trends in Analytical Chemistry 2014; 62:28-36
152. Chen Y, Xie Z, Zhang L, Hu X. Effective preparation of magnetic molecularly imprinted polymer nanoparticle for the rapid and selective extraction of cyfluthrin from honeysuckle. J Biomater Sci Polym Ed 2020.1-15
153. Lan T, Zhang J, Lu Y. Transforming the blood glucose meter into a general healthcare meter for in vitro diagnostics in mobile health. Biotechnol Adv 2016; 34:331-41
154. Devkota J, Howell M, Mukherjee P, Srikanth H, Mohapatra S, Phan MH. Magneto-reactance based detection of MnO nanoparticle-embedded Lewis lung carcinoma cells. J Appl Phys 2015; 117:17D123
155. Pankhurst Q, Connolly J, Jones S, Dobson J. Applications of magnetic nanoparticles in biomedicine. Journal of Physics D: Applied Physics 2003; 36:R167-R181
156. Clarke J, Lee YH, Schneiderman J. Focus on SQUIDs in Biomagnetism. Supercond Sci Technol 2018; 31:080201
157. Enpuku K, Tsujita Y, Nakamura K, Sasayama T, Yoshida T. Biosensing utilizing magnetic markers and superconducting quantum interference devices. Supercond Sci Tech 2017; 30:053002
158. Guo L, Yang Z, Zhi S, Feng Z, Lei C, Zhou Y. A sensitive and innovative detection method for rapid C-reactive proteins analysis based on a micro-fluxgate sensor system. PLoS One 2018; 13:e0194631
159. Heim E, Ludwig F, Schilling M. Binding assays with

streptavidin-functionalized superparamagnetic nanoparticles and biotinylated analytes using fluxgate magnetorelaxometry. Journal of Magnetism and Magnetic Materials 2009; 321:1628-1631
160. Krishna VD, Wu K, Perez AM, Wang JP. Giant Magnetoresistance-based Biosensor for Detection of Influenza A Virus. Front Microbiol 2016; 7:400
161. Ng E, Nadeau KC, Wang SX. Giant magnetoresistive sensor array for sensitive and specific multiplexed food allergen detection. Biosens Bioelectron 2016; 80:359-365
162. Wang Z, Hu T, Liang R, Wei M. Application of Zero-Dimensional Nanomaterials in Biosensing. Front Chem 2020; 8:320
163. Wang Y, Zhu Y, Huang J, Cai J, Zhu J, Yang X, Shen J, Li C. Perovskite quantum dots encapsulated in electrospun fiber membranes as multifunctional supersensitive sensors for biomolecules, metal ions and pH. Nanoscale Horiz 2017; 2:225-232
164. Mo G, Qin D, Jiang X, Zheng X, Mo W, Deng B. A sensitive electrochemiluminescence biosensor based on metal-organic framework and imprinted polymer for squamous cell carcinoma antigen detection. Sensors Actuators B: Chem 2020; 310:127852
165. Mandani S, Rezaei B, Ensafi AA. Sensitive imprinted optical sensor based on mesoporous structure and green nanoparticles for the detection of methamphetamine in plasma and urine. Spectrochim Acta A Mol Biomol Spectrosc 2020; 231:118077
166. Lofgreen JE and Ozin GA. Controlling morphology and porosity to improve performance of molecularly imprinted sol-gel silica. Chem Soc Rev 2014; 43:911-33
167. Gui R, Guo H, Jin H. Preparation and applications of electrochemical chemosensors based on carbon-nanomaterial-modified molecularly imprinted polymers. Nanoscale Advances 2019; 1:3325-3363
168. Lai CY, Trewyn BG, Jeftinija DM, Jeftinija K, Xu S, Jeftinija S, Lin VS. A mesoporous silica nanosphere-based carrier system with chemically removable CdS nanoparticle caps for stimuli-responsive controlled release of neurotransmitters and drug molecules. J Am Chem Soc 2003; 125:4451-9
169. Trewyn BG, Slowing II, Giri S, Chen H-T, Lin VS. Synthesis and Functionalization of a Mesoporous Silica Nanoparticle Based on the Sol-Gel Process and Applications in Controlled Release. Acc Chem Res 2007; 40:846-853
170. Vazquez NI, Gonzalez Z, Ferrari B, Castro Y. Synthesis of mesoporous silica nanoparticles by sol–gel as nanocontainer for future drug delivery applications. Boletín de la Sociedad Española de Cerámica y Vidrio 2017; 56:139-145
171. Amatatongchai M, Sitanurak J, Sroysee W, Sodanat S, Chairam S, Jarujamrus P, Nacapricha D, Lieberzeit PA. Highly sensitive and selective electrochemical paper-based device using a graphite screen-printed electrode modified with molecularly imprinted polymers coated Fe3O4@Au@SiO2 for serotonin determination. Anal Chim Acta 2019; 1077:255-265
172. Saeedzadeh Amiri N and Milani Hosseini M-R. Application of ratiometric fluorescence sensor-based microwave-assisted synthesized CdTe quantum dots and mesoporous structured epitope-imprinted polymers for highly efficient determination of tyrosine phosphopeptide. Analytical Methods 2020; 12:63-72
173. Geng Y, Guo M, Tan J, Huang S, Tang Y, Tan L, Liang Y. The fabrication of highly ordered fluorescent molecularly imprinted mesoporous microspheres for the selective sensing of sparfloxacin in biological samples. Sensors Actuators B: Chem 2019; 281:821-829
174. Kumar N, Chauhan NS, Mittal A, Sharma S. TiO2 and its composites as promising biomaterials: a review. Biometals 2018; 31:147-159
175. Sajini T, Gigimol MG, Mathew B. A brief overview of molecularly imprinted polymers supported on titanium dioxide matrices. Materials Today Chemistry 2019; 11:283-295
176. Zhao Z, Zhu C, Guo Q, Cai Y, Zhu X, Li B. Preparation of lysozyme-imprinted nanoparticles on polydopamine-modified titanium dioxide using ionic liquid as a stabilizer. RSC Advances 2019; 9:14974-14981
177. Huang X, Wei S, Yao S, Zhang H, He C, Cao J. Development of molecularly imprinted electrochemical sensor with reduced graphene oxide and titanium dioxide enhanced performance for the detection of toltrazuril in chicken muscle and egg. J Pharm Biomed Anal 2019; 164:607-614
178. Yu M, Wu L, Miao J, Wei W, Liu A, Liu S. Titanium dioxide and polypyrrole molecularly imprinted polymer nanocomposites based electrochemical sensor for highly selective detection of p-nonylphenol. Anal Chim Acta 2019; 1080:84-94
179. Zhang C, Bai W, Qin T, Yang Z. Fabrication of Red Mud/Molecularly Imprinted Polypyrrole-Modified Electrode for the Piezoelectric Sensing of Bilirubin. IEEE Sensors Journal 2019; 19:1280-1284
180. Erickson D, Mandal S, Yang AH, Cordovez B. Nanobiosensors: optofluidic, electrical and mechanical approaches to biomolecular detection at the nanoscale. Microfluid Nanofluidics 2008; 4:33-52
181. Xianyu YL, Wang QL, Chen YP. Magnetic particles-enabled biosensors for point-of-care testing. Trac-Trend Anal Chem 2018; 106:213-224
182. Wang SX and Li G. Advances in giant magnetoresistance biosensors with magnetic nanoparticle tags: Review and outlook. Ieee Transactions on Magnetics 2008; 44:1687-1702
183. Dey D and Goswami T. Optical biosensors: a revolution towards quantum nanoscale electronics device fabrication. J Biomed Biotechnol 2011; 2011:348218
184. Kausar AS, Reza AW, Latef TA, Ullah MH, Karim ME. Optical nano antennas: state of the art, scope and challenges as a biosensor along with human exposure to nano-toxicology. Sensors (Basel) 2015; 15:8787-831
185. Kidane S, Ishida H, Sawada K, Takahashi K. A suspended graphene-based optical interferometric surface stress sensor for selective biomolecular detection. Nanoscale Advances 2020; 2:1431-1436
186. Schrittwieser S, Pelaz B, Parak WJ, Lentijo-Mozo S, Soulantica K, Dieckhoff J, Ludwig F, Guenther A, Tschope A, Schotter J. Homogeneous Biosensing Based on Magnetic Particle Labels. Sensors (Basel) 2016; 16:
187. Lai M and Slaughter G. Label-Free MicroRNA Optical Biosensors. Nanomaterials (Basel) 2019; 9:

188. Sun Y and Zhong S. Molecularly imprinted polymers fabricated via Pickering emulsions stabilized solely by food-grade casein colloidal nanoparticles for selective protein recognition. Anal Bioanal Chem 2018; 410:3133-3143
189. Yousefzadeh A, Hassanzadeh J, Mousavi SMJ, Yousefzadeh M. Surface molecular imprinting and powerfully enhanced chemiluminescence emission by Cu nanoclusters/MOF composite for detection of tramadol. Sensors Actuators B: Chem 2019; 286:154-162
190. Zhao LF, Wei Q, Wu H, Li H, Li D, Mohapatra SS. Portable and quantitative evaluation of stem cell therapy towards damaged hepatocytes. Rsc Advances 2015; 5:19439-19444
191. Das A, Cui X, Chivukula V, Iyer SS. Detection of Enzymes, Viruses, and Bacteria Using Glucose Meters. Anal Chem 2018; 90:11589-11598
192. Wu T, Cao Y, Yang Y, Zhang X, Wang S, Xu LP, Zhang X. A three-dimensional DNA walking machine for the ultrasensitive dual-modal detection of miRNA using a fluorometer and personal glucose meter. Nanoscale 2019; 11:11279-11284
193. Jia X, Dong S, Wang E. Engineering the bioelectrochemical interface using functional nanomaterials and microchip technique toward sensitive and portable electrochemical biosensors. Biosens Bioelectron 2016; 76:80-90
194. Yuan L, Zhang J, Zhou P, Chen J, Wang R, Wen T, Li Y, Zhou X, Jiang H. Electrochemical sensor based on molecularly imprinted membranes at platinum nanoparticles-modified electrode for determination of 17beta-estradiol. Biosens Bioelectron 2011; 29:29-33
195. Amatatongchai M, Sroysee W, Jarujamrus P, Nacapricha D, Lieberzeit PA. Selective amperometric flow-injection analysis of carbofuran using a molecularly-imprinted polymer and gold-coated-magnetite modified carbon nanotube-paste electrode. Talanta 2018; 179:700-709
196. Yola ML and Atar N. Development of cardiac troponin-I biosensor based on boron nitride quantum dots including molecularly imprinted polymer. Biosens Bioelectron 2019; 126:418-424
197. Chen MM, Cheng SB, Ji K, Gao J, Liu YL, Wen W, Zhang X, Wang S, Huang WH. Construction of a flexible electrochemiluminescence platform for sweat detection. Chem Sci 2019; 10:6295-6303
198. Gu Y, Wang J, Shi H, Pan M, Liu B, Fang G, Wang S. Electrochemiluminescence sensor based on upconversion nanoparticles and oligoaniline-crosslinked gold nanoparticles imprinting recognition sites for the determination of dopamine. Biosens Bioelectron 2019; 128:129-136
199. Holzinger M, Le Goff A, Cosnier S. Synergetic Effects of Combined Nanomaterials for Biosensing Applications. Sensors (Basel) 2017; 17:
200. Chen GY, Thundat T, Wachter EA, Warmack RJ. Adsorption-induced surface stress and its effects on resonance frequency of microcantilevers. Journal of Applied Physics 1995; 77:3618-3622
201. Wang T, Green R, Nair RR, Howell M, Mohapatra S, Guldiken R, Mohapatra SS. Surface Acoustic Waves (SAW)-Based Biosensing for Quantification of Cell Growth in 2D and 3D Cultures. Sensors (Basel) 2015; 15:32045-55
202. Yu H, Chen Y, Xu P, Xu T, Bao Y, Li X. mu-'Diving suit' for liquid-phase high-Q resonant detection. Lab Chip 2016; 16:902-10
203. Mazouz Z, Rahali S, Fourati N, Zerrouki C, Aloui N, Seydou M, Yaakoubi N, Chehimi MM, Othmane A, Kalfat R. Highly Selective Polypyrrole MIP-Based Gravimetric and Electrochemical Sensors for Picomolar Detection of Glyphosate. Sensors (Basel) 2017; 17:
204. Okan M, Sari E, Duman M. Molecularly imprinted polymer based micromechanical cantilever sensor system for the selective determination of ciprofloxacin. Biosens Bioelectron 2017; 88:258-264
205. Dayal H, Ng WY, Lin XH, Li SFY. Development of a hydrophilic molecularly imprinted polymer for the detection of hydrophilic targets using quartz crystal microbalance. Sensors Actuators B: Chem 2019; 300:127044
206. Tang P, Wang Y, Huo J, Lin X. Love Wave Sensor for Prostate-Specific Membrane Antigen Detection Based on Hydrophilic Molecularly-Imprinted Polymer. Polymers (Basel) 2018; 10:
207. Dezest D, Leïchlé T, Teerapanich P, Mathieu F, Bui BTS, Haupt K, Nicu L. Multiplexed functionalization of nanoelectromechanical systems with photopatterned molecularly imprinted polymers. Journal of Micromechanics and Microengineering 2019; 29:025013